HHS Public Access

Author manuscript

Cell Rep. Author manuscript; available in PMC 2019 May 22.

Published in final edited form as:

Cell Rep. 2019 April 30; 27(5): 1446–1460.e4. doi:10.1016/j.celrep.2019.04.019.

FCRL5^{+} Memory B Cells Exhibit Robust Recall Responses

Charles C. Kim[1,3], **Alyssa M. Baccarella**[1], **Aqieda Bayat**[1], **Marion Pepper**[2], and **Mary F. Fontana**[1,2,4,*]

[1]Division of Experimental Medicine, Department of Medicine, University of California, San Francisco, San Francisco, CA 94143, USA

[2]Department of Immunology, University of Washington School of Medicine, Seattle, WA 98109, USA

[3]Present address: Verily, South San Francisco, CA 94080, USA

[4]Lead Contact

SUMMARY

FCRL5^{+} atypical memory B cells (atMBCs) expand in many chronic human infections, including recurrent malaria, but studies have drawn opposing conclusions about their function. Here, in mice infected with *Plasmodium chabaudi*, we demonstrate expansion of an antigen-specific FCRL5^{+} population that is distinct from previously described FCRL5^{+} innate- like murine subsets. Comparative analyses reveal overlapping phenotypic and transcriptomic signatures between FCRL5^{+} B cells from *Plasmodium*-infected mice and atMBCs from *Plasmodium*-exposed humans. In infected mice, FCRL5 is expressed on the majority of antigen-specific germinal-center-derived memory B cells (MBCs). Upon challenge, FCRL5^{+} MBCs rapidly give rise to antibody-producing cells expressing additional atypical markers, demonstrating functionality *in vivo*. Moreover, atypical markers are expressed on antigen-specific MBCs generated by immunization in both mice and humans, indicating that the atypical phenotype is not restricted to chronic settings. This study resolves conflicting interpretations of atMBC function and suggests FCRL5^{+} B cells as an attractive target for vaccine strategies.

Graphical Abstract

*Correspondence: mfontana@uw.edu.

AUTHOR CONTRIBUTIONS

Conceived of the Project, C.C.K., M.P., and M.F.F. Designed Experiments, C.C.K., M.P., and M.F.F. Performed Experiments, C.C.K., A.M.B., A.B., and M.F.F. Analyzed Data, C.C.K., A.M.B., A.B., M.P., and M.F.F. Wrote the Paper: M.F.F. with M.P.

SUPPLEMENTAL INFORMATION

Supplemental Information can be found online at https://doi.org/10.1016/j.celrep.2019.04.019.

DECLARATION OF INTERESTS

The authors declare no conflicts of interest.

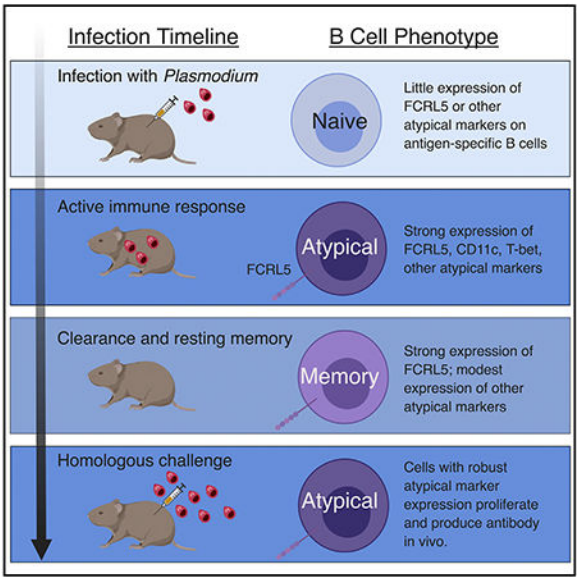

In Brief

FCRL5^{+} atypical memory B cells (MBCs) expand in many chronic human diseases. Using tetramers to track rare antigenspecific cells, Kim et al. show that FCRL5^{+}MBCs are mature, optimally responsive cells that arise not only in response to infection and protein immunization in mice but also to immunization in humans.

INTRODUCTION

Humoral immunity entails the generation of long-lived B cell populations consisting of antibody-secreting plasma cells and memory B cells (MBCs) that can quickly differentiate into plasmablasts upon challenge (Harms Pritchard and Pepper, 2018). In chronic infections, however, although robust B cell responses may form, they are apparently insufficient to achieve microbial clearance. In this context, it has been proposed that prolonged stimulation may result in B cell dysfunction, akin to the exhaustion that occurs in chronically stimulated T cells (Moir and Fauci, 2014; Moir et al., 2008; Wherry et al., 2007). Despite their failure to clear infection, ongoing immune responses may nevertheless keep chronic pathogen burdens in check, as demonstrated by observations that exhausted T cells contribute to the restriction of chronic viral infection (Speiser et al., 2014; Wherry and Kurachi, 2015).

Over the last 10 years, studies have identified a population of MBCs that expands in a number of chronic infections in humans, including hepatitis C virus (HCV), HIV, and malaria (Charles et al., 2011; Moir et al., 2008; Portugal et al., 2015; Sullivan et al., 2015; Weiss et al., 2009), as well as in autoimmune settings such as lupus (Jacobi et al., 2008). Called atypical MBCs (atMBCs) or exhausted or tissue-like B cells, they can be distinguished from classical MBCs (cMBCs) by lack of expression of the memory markers CD21 and CD27 and by expression of a number of putative inhibitory receptors, including Fc receptor-like (FCRL) 3, 4, and 5 (Moir et al., 2008; Portugal et al., 2015; Sullivan et al., 2015). Because of their association with ongoing infections, it has been proposed that

atMBCs are functionally defective. Consistent with this notion, two studies have shown that atMBCs from humans with chronic *Plasmodium* exposure exhibit impaired proliferation and antibody production upon re-stimulation *ex vivo*, relative to cMBCs (Portugal et al., 2015; Sullivan et al., 2015). Yet a dissenting study drew the opposite conclusion, presenting evidence that these cells proliferate robustly *in vivo* and contribute as much as cMBCs to serum antibody levels (Muellenbeck et al., 2013). Thus the functional capacity of atMBCs, as well as their role in protective immunity, remains poorly understood and is difficult to dissect in humans.

In this work, we characterize a population of FCRL5$^+$ B cells that expands during infection of mice with *Plasmodium chabaudi*, a rodent-tropic parasite that is commonly used to model uncomplicated infection with the principal etiological agent of human malaria, *Plasmodium falciparum* (Stephens et al., 2012). These B cells bear numerous phenotypic and transcriptional similarities to human atMBCs from individuals with chronic *P. falciparum* exposure and respond robustly to secondary challenge. Our data suggest that FCRL5$^+$ MBCs are not dysfunctional but instead are a mature and responsive memory population.

RESULTS

P. chabaudi Infection Elicits Expansion of an FCRL5$^+$ B Cell Subset

In humans, atMBCs are defined by the absence of the cMBC markers CD21 and CD27 (Ehrhardt et al., 2005; Moir et al., 2008; Portugal et al., 2015; Sullivan et al., 2015; Weiss et al., 2009). Downregulation of CD21 and CD27 can be associated with activation, raising questions about the identity of this population (Agematsu et al., 1997; Masilamani et al., 2003). To facilitate experimental characterization of atMBCs, we asked whether an analogous population of B cells develops in an animal model. Recently, we and others demonstrated that the surface receptors FCRL3 and FCRL5 are preferentially expressed by atMBCs from human subjects chronically exposed to *P. falciparum* (Portugal et al., 2015; Sullivan et al., 2015). Therefore, we examined whether FCRL receptors could be used to define an atMBC-like subset in mice infected with *Plasmodium*.

The mouse gene *Fcrl5* possesses significant sequence and domain homology to both human FCRL5 and human FCRL3, whereas its cellular expression patterns resemble those of human FCRL3 (Li et al., 2014). FCRL5 is known to be expressed in murine B-1 cells and human B-1 and B-2 cells and may play either an activating or an inhibitory role depending on its context (Franco et al., 2018; Li et al., 2014; Rakhmanov et al., 2009; Zhu et al., 2013). Yet, little is known about FCRL5 expression and function in murine B-2 cells. To identify cells analogous to the atMBCs found in human blood after *P. falciparum* infection, we tracked the expression of FCRL5 on blood B cells from mice infected with *P. chabaudi* (Figure 1A). During blood-stage infection, parasitemia (% of red blood cells infected) peaks approximately 7 days post-infection (d.p.i.), after which it is rapidly controlled by the host immune response, falling below the limit of microscopic detection by 3 to 4 weeks post-infection (Figure 1B, solid line). During this time, we observed a transient increase in the frequency of FCRL5$^+$ B cells in the blood, from approximately 10% of B cells at the time of infection to ~40% several weeks post-infection. A similar expansion was observed in the spleen (Figure 1B, dashed lines). A related parasite strain, *Plasmodium yoelii*, also elicited

transient expansion of FCRL5$^+$ B cells (Figure S1A). Thus, acute *Plasmodium* infection increases the frequency of FCRL5$^+$ B cells in mice as well as humans (Scholzen et al., 2014; Sullivan et al., 2016).

FCRL5$^+$ B Cells in Infected Mice Are Distinct from Innate-like B Cells

In contrast to the literature on chronic human infection, previous studies in mice have characterized FCRL5 primarily as a marker of innate-like B cells, including splenic marginal zone B cells (MZB) and peritoneal B-1 cells (Davis, 2015). We therefore assessed levels of CD11b, CD5, and CD1d, markers of body cavity B-1 cells, B-1a cells, and MZB, respectively (Roark et al., 1998; Haas et al., 2005). FCRL5$^+$ B cells from the blood of mice 21 d.p.i. did not express CD1d or CD5, suggesting that they are neither MZB nor B-1a cells. FCRL5$^+$ blood B cells did express more CD11b than FCRL5$^-$ B cells; however, their average expression was markedly lower than that of peritoneal cavity B-1 cells. In addition, FCRL5 itself was expressed at lower levels on FCRL5$^+$ blood B cells from infected mice relative to its expression on MZB or peritoneal B-1 cells (Figure 1C). Because body cavity B-1a cells have been shown to migrate into secondary lymphoid organs upon influenza infection (Choi and Baumgarth, 2008; Waffarn et al., 2015), we specifically assessed whether the FCRL5$^+$ B cells we observed during *Plasmodium* infection were B-1a cells trafficking through the blood. B-1a cells were detected, but made up only a small fraction (<1%) of the total FCRL5$^+$ population in the blood (Figures 1D) and 1E. To further test whether FCRL5 could be expressed inducibly on B-2 cells during *P. chabaudi* infection, we sorted FCRL5$^-$ CD23$^+$ CD21^{lo} splenic follicular B cells from naive CD45.1$^+$/CD45.2$^+$ mice and transferred them into congenic CD45.2$^+$ mice prior to infection. A substantial fraction of transferred B cells upregulated FCRL5 following infection, demonstrating that FCRL5$^-$ follicular B cells can give rise to FCRL5$^+$ B cells in mice with malaria (Figure S1B). Together, these data support the conclusion that the expanded population of FCRL5$^+$ B cells in infected mice is distinct from innate-like FCRL5$^+$ B cell subsets.

Transcriptional Profiling Identifies Similarities between Inducible FCRL5$^+$ Murine B Cells and Human atMBCs

We previously reported that *Ifngr1*$^{-/-}$ mice chronically infected with *P. chabaudi* (patent parasitemia persisting >100 days) develop high frequencies of class-switched FCRL5$^+$ B cells in the blood (Fontana et al., 2016). To build on this observation, we performed global transcriptional profiling on class-switched, FCRL5$^+$ or FCRL5$^-$B cells sorted from acutely infected *Ifngr1*$^{-/-}$ mice 21 d.p.i., when FCRL5$^+$ cells are abundant in circulation (gating in Figure S2). RNA sequencing (RNA-seq) analysis revealed that FCRL5$^+$ and FCRL5$^-$B cells express distinct transcriptional signatures, with significant differences in 265 genes, or 2.5% of the 10,765 reliably detected transcripts (Table S1). Like atMBCs (Portugal et al., 2015; Sullivan et al., 2015), FCRL5$^+$ B cells exhibited increased expression of several receptors and downstream adaptors with inhibitory or immunosuppressive functions (*Cd72*, *Entpd1*, *Lgals1*, *Lilrb3*, and *Lyn*) and decreased expression of several B cell receptor (BCR) signaling components (*Ighg1*, *Syk*, and *CD79b*) and receptors that pro- mote activation, differentiation, and/or survival (*Il2rg*, *Cd83*, *Tnfrsf13c*, and *Il21r*) (Figure 2A). Consistent with these observations, functional enrichment analysis (Dennis et al., 2003) identified cell surface proteins and integrin-mediated signaling path- ways among the gene categories that

displayed differential expression between the two subsets (Table S2). Bioinformatic comparison with previously published transcriptional profiles from atMBCs in *Plasmodium*-exposed humans (Sullivan et al., 2015) identified 34 genes whose pattern of expression is similar in both human atMBCs and FCRL5^{+} mouse B cells, relative to human cMBCs and FCRL5^{-}B cells, respectively (Figure 2B). These genes represent approximately 13% of the genes that are differentially regulated in FCRL5^{+} versus FCRL5^{-}B cells from infected mice. To test whether this overlap was meaningful, we calculated the cumulative probability that it would occur by chance. We found that the overlap between differentially ex- pressed genes in FCRL5^{+} murine B cells and those exhibiting similar differential expression in human atMBCs (e.g., both upregulated) was highly statistically significant (hypergeometric p value = 2×10^{-5}). Comparisons with existing meta-analyses that assess the similarity of tissue-specific gene signatures between mice and humans (e.g., Zheng-Bradley et al., 2010) suggest that this level of transcriptional similarity likely does imply biological similarity between the cell subsets. In further support of this conclusion, a recent study that performed transcriptional profiling on *Plasmodium*-specific transgenic B cells in mice infected with *P. chabaudi* also found evidence for a relationship between murine cells expressing atypical markers and human atMBCs (Pérez-Mazliah et al., 2018).

We used flow cytometry in wild-type mice to confirm differen- tial protein expression of several genes identified by RNA-seq (*Cd72*, *Cd38*, and *Itgam*, encoding CD11b; Figures 2C and 2E). Of note, the gene *Tbx21*, which encodes the transcription factor T-bet, was upregulated in both human atMBCs (Sullivan et al., 2015; Obeng-Adjei et al., 2017) and mouse FCRL5^{+} B cells 21 d.p.i. (Figures 2A and 2B), an observation we confirmed at the protein level (Figure 2D).

In addition to its expression in atMBCs, T-bet is expressed in age-associated B cells (ABCs), a subset characterized in mice that bears similarity to atMBCs (Hao et al., 2011; Rubtsov et al., 2011; Rubtsova et al., 2015). Compared to FCRL5^{-}cells, FCRL5^{+} B cells taken from *Plasmodium*-infected mice 21 d.p.i. upregulated CD11b and CD11c, defining markers of ABCs, as well as CD86 and CD40, which are upregulated on atMBCs in malaria and other settings (Figure 2E) (Ehrhardt et al., 2005; Weiss et al., 2009; Rubtsov et al., 2011; Hao et al., 2011; Sullivan et al., 2015). Together, these transcriptional and phenotypic analyses support the hypothesis that the inducible FCRL5^{+} population we observe in acutely infected mice is analogous to the atMBCs that develop in human *Plasmodium* infection. They also reinforce the previously noted resemblance between atMBCs and ABCs (Rubtsova et al., 2015).

Expression of FCRL5 on Antigen-Speci1fic MBCs

To examine FCRL5 expression specifically on MBCs, we employed techniques to label and enrich antigen-specific B cells from *Plasmodium*-infected mice. *Plasmodium*-specific B cells were identified using a fluorescently tagged tetramer reagent incorporating a truncated portion of the carboxy terminus of the *P. chabaudi* blood-stage antigen merozoite surface protein 1 (MSP1) (Krishnamurty et al., 2016). A decoy reagent was used to exclude B cells that bound to components of the tetramer other than MSP1 (Taylor et al., 2012). MSP1-specific cells expanded several-fold in the spleen following infection and a fraction

expressed FCRL5; the proportion of FCRL5$^+$ cells increased from ~30% of all MSP1-specific cells in naive mice to ~50% measured 110 d.p.i. (Figure 3A). Detection of FCRL5 on antigen-specific cells persisting months after infection further supports the contention that these FCRL5$^+$ cells are not a previously described innate-like population but rather include bona fide MBCs.

We examined the expression of FCRL5 on various antigen-specific B cell subsets. In a recent study, transcriptional profiling led the authors to suggest that FCRL5$^+$ MSP1-specific B cells expressed a plasmablast- or pre-plasmablast-like signature, but cell surface markers for plasmablasts were not assessed (Pérez- Mazliah et al., 2018). Therefore, we examined antigen-specific B cells for expression of these and other subset markers.

Whereas CD138$^-$MSP1-specific B cells in infected mice could be resolved into distinct FCRL5$^+$ and FCRL5$^-$ populations, CD138$^+$ plasma cells or plasmablasts uniformly exhibited low-to-intermediate FCRL5 expression with a median fluorescent intensity (MFI) only slightly higher than that of the FCRL5$^-$ CD138$^-$ population (Figure 3B). CD138$^+$ cells examined 28 d.p.i. were uniformly B220^{lo}, indicating differentiation into plasma cells (Figure 3C), but similar results were obtained at earlier time points when B220^{hi} plasmablasts were present. Antigen-specific germinal center (GC) B cells (defined as B220^{hi} CD138$^-$ GL7$^+$ CD38$^-$) did not express FCRL5 at any time point examined (Figure 3D). Cells not falling into either of these subsets were considered to be a combined naive and MBC pool because markers to distinguish unambiguously between naive and memory cells are lacking in the mouse. FCRL5$^+$ cells in the MSP1-specific memory-naive gate (B220^{hi} CD138$^-$ CD38$^+$ GL7$^-$) expressed higher levels of CD38 relative to FCRL5$^-$ cells, suggestive of a memory phenotype (Figure 3E). They also had higher side scatter than FCRL5$^-$ cells, echoing morphological observations of CD21$^-$ CD27$^-$ FCRL4$^+$ MBCs in human tonsils (Figure 3F) (Ehrhardt et al., 2005). Similar to bulk FCRL5$^+$ B cells (Figure 2D), antigen-specific FCRL5$^+$ B cells expressed increased levels of T-bet 28 d.p.i. (Figure 3G) as well as increased CD11b, CD11c, and CD86, all markers of atMBCs or ABCs (Figure 3H). Together, these data demonstrate that FCRL5 is expressed on antigen- specific MBCs with numerous similarities to human atMBCs but is low or absent on GC B cells, plasma cells, and plasma- blasts generated during primary infection.

FCRL5 Expression Is Associated with IgD Downregulation and Memory Maturation

P. chabaudi induces long-lived antigen-specific MBCs that can be divided into three populations by isotype: immunoglobulin D (IgD)$^+$ B cells, which have varying levels of immunoglobulin M (IgM) expression; IgM$^+$ IgD$^-$cells (referred to hereafter as IgM$^+$), and IgD$^-$IgM$^-$cells, referred to here as SwIg, which have class-switched and which in malaria are likely to express immunoglobulin G (IgG) (Krishnamurty et al., 2016). In humans, atMBCs may express either IgM or IgG (Krishnamurty et al., 2016; Sullivan et al., 2015; Weiss et al., 2009). We examined FCRL5 levels on IgD$^+$, IgM$^+$, and SwIg MSP1-specific cells from the memory-naive gate (B220^{hi} CD138$^-$CD38$^+$ GL7$^-$) 28 d.p.i. and found a strong association between downregulation of IgD and expression of FCRL5, with ~75% of SwIg cells positive for FCRL5 28 d.p.i. compared to ~22% of IgD$^+$ B cells. IgM$^+$ cells displayed intermediate FCRL5 expression (~45%; Figure 4A). Throughout infection, the

majority of MSP1-specific IgD^+ memory-naive cells remained $FCRL5^-$, whereas antigen-specific IgM^+ and SwIg MBCs shifted increasingly into the $FCRL5^+$ subset over time (Figure 4B). By 110 d.p.i., virtually all SwIg cells (Figure 4C) and over half of IgM^+ B cells (Figure 4D) expressed FCRL5, indicating that this receptor marks long-lived, antigen-specific MBCs, especially those that have downregulated IgD.

Previous work from our group has shown that *Plasmodium* infection elicits both IgM^+ and SwIg MSP1-specific MBCs ex- pressing the maturation markers CD73 and CD80 (Krishnamurty et al., 2016), which are upregulated on rapidly responsive MBCs (Tomayko et al., 2010; Taylor et al., 2012). CD80 is also upregulated on atMBCs in *Plasmodium*-exposed humans (Zuccarino- Catania et al., 2014). $CD73^+$ $CD80^+$ MSP1-specific MBCs were readily detected in infected mice; notably, virtually all expressed FCRL5 (Figure 4E). Although all $CD73^+$ $CD80^+$ MBCs expressed FCRL5, a sizeable fraction of $FCRL5^+$ cells did not express CD73 or CD80 (Figure 4F). We hypothesized that these cells may be either GC-independent MBCs or naive cells; consistent with this, most $FCRL5^+$ cells that lacked CD73 and CD80 were IgD^+, whereas approximately half of $FCRL5^+$ IgM^+ MBCs ex-pressed CD73 and CD80 and nearly all SwIg MBCs expressed all three of these markers (Figure S3A). Thus, despite its absence in the GC, FCRL5 is greatly enriched on B cells exhibiting robust maturation phenotypes, including persistence after infection, downregulation of IgD, and expression of CD73 and CD80, all of which suggest that they are GC-derived and/or T cell dependent.

Previous work has demonstrated a requirement for T-bet in the formation of antigen-specific ABCs during viral infection (Rubtsova et al., 2013); therefore, we wondered whether it was also required for differentiation of $FCRL5^+$ MBCs during malaria. We were somewhat surprised to find that mice lacking T-bet specifically in B cells (*Mb1-Cre*; $Tbx21^{fl/fl}$) displayed no defect in the frequencies or overall isotype distribution (IgM^+ versus SwIg) of $FCRL5^+$ MBCs following *P. chabaudi* infection, indicating that T-bet is not required for their development (Figures S3B) and S3C. T-bet has been shown to skew IgG isotypes toward IgG2a (Rubtsova et al., 2013); thus, it is possible that deletion of T-bet alters the distribution of IgG subtypes in *Plasmodium* infection without affecting the overall frequency of SwIg cells.

Expression of FCRL5 on MBCs Responding to Acute Infection or Immunization

As murine infection with *P. chabaudi* results in a sub-patent parasitemia that persists as long as 3 months (Stephens et al., 2012), it is possible that the population of $FCRL5^+$ memory cells that form in this infection are not representative of cMBCs. To test this, we generated additional B cell tetramers to examine anti- gen-specific $FCRL5^+$ MBCs during either acute viral infection or protein immunization. The B cell response to infection with the Armstrong strain of the lymphocytic choriomeningitis virus (LCMV), which is cleared by approximately a week after infection, could be tracked with tetramers incorporating the viral glycoprotein (GP) (Figure 5A). Six weeks after infection, an expanded population of $B220^{hi}$ $CD138^-CD38^+$ $GL7^-$GP-specific MBCs exhibited a very similar phenotype to those from *Plasmodium* infection, with over half of IgM^+ GP-specific cells and the majority of SwIg cells expressing FCRL5 (Figure 5B). As in *Plasmodium* infection, virtually all $CD73^+$

CD80$^+$ GP-specific MBCs elicited by LCMV also expressed FCRL5 (Figure 5C). Thus, FCRL5 is expressed on antigen-specific, GC-derived MBCs induced by an acute infection, indicating that its expression is not limited to settings with chronic antigen stimulation.

To test whether FCRL5 expression is upregulated on MBCs elicited by immunization, we also examined ovalbumin (OVA)- specific B cells in spleens of mice immunized with OVA in aluminum hydroxyl (alum) (Figure 5D). Gating on OVA-specific memory-naive B cells 21 days after immunization again revealed a large portion of MBCs expressing FCRL5. In contrast to LCMV and *Plasmodium* infections, however, most FCRL5$^+$ cells were IgM$^+$, whereas the majority of SwIg cells were FCRL5$^-$(Figure 5E) despite expression of CD73 and CD80 (Figure 5F). Together with the LCMV data, these experiments indicate that FCRL5 is expressed on CD73$^+$ CD80$^+$ MBCs in diverse immune settings but that different stimuli can elicit distinct patterns of expression.

FCRL5$^+$ MBCs Make Robust Recall Responses

Previous studies have suggested that atMBCs from humans with repeated *Plasmodium* exposure may be dysfunctional because they give rise to fewer antibody-secreting cells than do cMBCs when restimulated *ex vivo* (Portugal et al., 2015; Sullivan et al., 2015). However, our group has demonstrated that MSP1-specific MBCs expressing CD73 and CD80 respond robustly to challenge (Krishnamurty et al., 2016), raising the possibility that FCRL5$^+$ MBCs exhibit good recall responses *in vivo*. To test the functional capacity of FCRL5$^+$ MBCs in mice, we first sorted MSP1-specific MBCs (B220^{hi} CD138$^-$CD38$^+$ GL7$^-$IgD$^-$) 3 months post-infection on the basis of FCRL5 expression and then restimulated cells *ex vivo* for 3 days, a time frame in which MBCs but not naive cells develop into antibody-secreting cells (Krishnamurty et al., 2016). EliSPOTs capturing both IgM and IgG responses revealed that FCRL5$^+$ B cells gave rise to as many antibody-secreting cells as FCRL5$^-$B cells, indicating they are fully competent for rapid differentiation into plasma- blasts (Figure 6A).

It was also important to examine how these cells respond *in vivo*. Mice were, therefore, infected with *P. chabaudi*, rested for 4 months, and then challenged with homologous parasites to measure functional responsiveness by both proliferation and antibody production after 5 days, a time at which we have shown that the majority of responses arise from memory rather than naive B cells (Krishnamurty et al., 2016).

To assess the recall capacity of FCRL5$^+$ MBCs, we first examined changes in the MBC compartment (B220^{hi} CD138$^-$CD38$^+$ GL7$^-$IgH+L^{lo}) before and after challenge. In “memory” mice, which were infected and rested but not challenged, a majority of IgM$^+$ and SwIg MBCs (55%–60%) expressed FCRL5. Assessing Ki67 expression as a readout of cellular proliferation, we found that whereas FCRL5$^-$MBCs of each isotype had slightly elevated Ki67 levels in resting mice, the FCRL5$^+$ MBCs were Ki67$^-$(Figure 6B), consistent with the quiescence we would expect in bona fide MBCs (Jones et al., 2015). Challenge with *P. chabaudi* resulted in proliferation of FCRL5$^+$ MBCs but not of FCRL5$^-$MBCs, as evidenced by increased Ki67 expression in the former; this was true for both IgM$^+$ and SwIg subclasses (Figures 6B, 6C, and S4). Thus, FCRL5$^+$ MBCs represent both the quiescent population in memory mice and the principle re- sponders, measured by increased proliferation, in challenged mice.

We next examined CD138^{+} antibody-secreting cells, which were scarce in memory mice but increased in abundance after secondary challenge (Figure 6D). The CD138^{+} population could be subdivided into CD138^{int} cells that co-expressed FCRL5, as well as CD138^{hi} cells that were FCRL5^{-}(Figure 6E). The FCRL5^{+} CD138^{int} population exhibited high B220 and relatively low intracellular IgH+L expression, consistent with the pheno- type of newly emerging plasmablasts (Hayakawa et al., 1987), whereas the FCRL5^{-}CD138^{hi} subset consisted of fully differentiated antibody-secreting cells that had ramped up intracellular IgH +L production and downregulated B220 (Figures 6F–6H). Intracellular antibody levels were slightly increased in FCRL5^{+} CD138^{+} cells relative to all CD138^{-}cells (Figure 6H), supporting the notion that these cells are transitioning toward antibody production. Together, the data are consistent with a model in which FCRL5^{+} MBCs selectively proliferate upon challenge, thereby both amplifying the memory pool (which retains FCRL5 expression) and also giving rise to the majority of CD138^{+} antibody- secreting cells, which gradually downregulate FCRL5 along with B220 as they differentiate. Our results suggest that FCRL5^{+} MBCs are not dysfunctional but in fact are the principal responders to secondary challenge.

Transient Expression of Other Atypical Markers on Long-Lived FCRL5^{+} MBCs

Because several markers expressed on human atMBCs are broadly associated with B cell activation (e.g., CD80, CD86, and CD11c), a key question is whether the atypical phenotype represents a stable cellular identity or rather a transient activation state. In their study of BCR-transgenic mice infected with *P. chabaudi*, Pérez-Mazliah et al. (2018) show that many MSP1-specific B cells robustly express atypical markers 35 d.p.i., a time when parasites are still present; our data from day 28 replicate these findings (Figure 3H). In contrast, they report that at day 155, several months after the infection has been cleared, antigen-specific MBCs express FCRL5 but not the other markers examined (CD11b, CD11c, and T-bet).

To test whether the expression of these markers is transient in our model as well, we examined MSP1-specific cells 150 d.p.i., looking specifically at IgD^{-}cells to enrich for memory over naive B cells. A side-by-side comparison of mice infected for either 28 or 150 days confirmed that the expression intensity of FCRL5 remained consistent over time (Figures 7A and 7B), whereas the intensity (MFI) of CD11b, CD11c, and T-bet was reduced on IgD^{-}antigen-specific MBCs at day 150 relative to expression on day 28 (Figure 7C). On day 150, approximately 2 months after parasite clearance, we still observed significantly elevated levels of CD11b, CD11c, and T-bet on antigen-specific IgD^{-}FCRL5^{+} cells relative to FCRL5^{-}cells, but the effect was modest and may have been driven by a small number of cells retaining robust expression (Figure 7C).

We expanded our measurements of CD11b and CD11c expression to include MBCs in other immune settings. Both markers were elevated on FCRL5^{+} OVA-specific and GP-specific cells elicited by protein immunization and LCMV expression, respectively (Figure S5), but expression was reduced compared to a similar time point after *Plasmodium* infection (Figure 7C). It seems likely that CD11b and CD11c are more transiently ex- pressed following immunization and even acute viral infection compared to *P. chabaudi* infection, in which parasites persist for months; in keeping with this, Pérez-Mazliah et al. (2018) report that

injection of MSP1 protein with a Toll-like receptor 7/8 (TLR7/8) ligand elicits a transient population of $CD11b^+$ $CD11c^+$ antigen-specific B cells that peaks 24 h post-immunization. Together with observations from *P. chabaudi*, these data suggest that some atypical markers diminish over time, and that their expression intensity correlates with recency of activation.

Returning to the *P. chabaudi* model, we assessed how expression of atypical markers would change on MBCs during a secondary response. We compared antigen-specific B cells from memory mice, which were infected and rested for 150 days but not challenged, to cells from mice that were challenged with *P. chabaudi* 150 d.p.i. To further ensure that we were assessing memory rather than naive responses, we analyzed splenocytes *ex vivo* 3 days after challenge, a time when the response from naive B cells is negligible (Figure S6A; Krishnamurty et al., 2016). We first examined antibody-producing cells ($CD138^+$ $IgH+L^{hi}$). Comparison with $CD138^-$B cells (which included memory, naive, and GC populations) revealed that the $CD138^+$ population elicited by challenge was $FCRL5^+$, consistent with our data from the 5-day challenge, suggesting that secondary plasmablasts differentiate from $FCRL5^+$ MBCs (Figures 6D–6H). Furthermore, they exhibited strong expression of CD11b and CD11c (Figure 7D). Measurement of robust intracellular antibody production in these cells, which are derived from recently re-activated MBCs and express multiple atypical markers, provides confirmation that cells with the atypical phenotype are fully functional and responsive to challenge.

Next, we examined IgD^-MBCs and found that the $FCRL5^+$ subset displayed higher CD11c and CD11b expression than its $FCRL5^-$counterpart in both control and challenged mice. Com- parison of $FCRL5^+$ cells before and after challenge suggested a trend toward increased CD11b and CD11c expression in the memory compartment after challenge, but the increase was not statistically significant, perhaps because the most highly activated cells have differentiated into plasmablasts by this time (Figures 7E, 7F, and S6B). Taken together, these data demonstrate that during a secondary response, reactivated MBCs and especially MBC-derived plasmablasts express an atypical surface phenotype while responding robustly to challenge.

Antigen-Specific $CD21^+$ $CD27^+$ MBCs from Humans Express Atypical Markers

Our data from the mouse model suggest that atMBCs are in fact long-lived, GC-derived, fully functional MBCs or MBC-derived antibody-secreting cells. To relate this hypothesis back to human biology, we used tetramers to enrich B cells specific for the tetanus toxoid C fragment (TTCF), a component of the tetanus vaccine, from human peripheral blood mononuclear cells (PBMCs). Because most American adults have received a tetanus vaccine (and very few are likely to have been exposed to this antigen by infection), we infer that TTCF-specific MBCs from healthy adult PBMCs are likely to arise from vaccination, an acute stimulus that has not been linked to development of atMBCs.

First, to validate our antibody panel on bulk (non-antigenspecific) B cells, we confirmed that a sizeable fraction of $CD21^-CD27^-$atMBCs expressed the atypical markers FCRL5 and CD11c, whereas expression was limited on $CD21^+$ $CD27^+$ cMBCs, consistent with published literature (Figure 7G). We next examined TTCF-specific B cells. Of these, ~90% expressed the memory marker CD27, and approximately 50% had the classical $CD21^+$

$CD27^+$ MBC phenotype, although substantial frequencies of $CD21^-CD27^+$ antigen-specific cells were also detected in some donors. The fraction of B cells that expressed CD27 (either with or without CD21 co-expression) was significantly higher in the TTCF-specific pool than in the bulk B cell population, confirming enrichment for MBCs (Figure 7H).

We examined TTCF-specific MBCs for expression of the atMBC markers CD11c and FCRL5. Whereas $CD21^+$ $CD27^+$ cells from the bulk B cell population had a very low proportion of $FCRL5^+$ $CD11c^+$ cells, antigen-specific $CD21^+$ $CD27^+$ B cells displayed significant co-expression of these markers (Figure 7I). FCRL5 and CD11c co-expression was even more prevalent on antigen-specific $CD21^-CD27^+$ B cells, which are thought to be recently activated MBCs. In contrast, bulk $CD21^-CD27^+$ B cells had minimal expression. Importantly, the $FCRL5^+$ $CD11c^+$ TTCF- specific B cells we observed in healthy humans were presumably elicited by an acute rather than a chronic stimulus (i.e., vaccination), and most had a classical $CD21^+$ $CD27^+$ MBC phenotype. These data provide further evidence that markers that have been previously associated with an atypical and potentially even dysfunctional B cell phenotype are in fact expressed on normal, long-lived, antigen-specific MBCs in both mice and humans and are not unique to chronic settings.

DISCUSSION

Acquisition of protective immunity to malaria is inefficient, requiring years and many repeated exposures to develop (Ryg-Cornejo et al., 2016; Schofield and Mueller, 2006). Accordingly, it is of great interest to understand whether the atMBCs that arise in malaria (as well as in other chronic infections) underlie this apparent failure of immunity (Portugal et al., 2013; Ryg-Cornejo et al., 2016). Because different studies have come to opposing conclusions on atMBC function (Moir et al., 2008; Muellenbeck et al., 2013; Portugal et al., 2015; Sullivan et al., 2015; Wang et al., 2018), it has been critical to identify an analogous population in animal models.

Several lines of evidence support the contention that $FCRL5^+$ murine MBCs are analogous to human atMBCs. Following a single *Plasmodium* infection, both populations expand in the blood and then contract as infection is cleared (Figure 1C; Scholzen et al., 2014; Sullivan et al., 2016), whereas chronic or repeated infection leads to a sustained increase in frequency (Fontana et al., 2016; Weiss et al., 2009). When examined during acute infection, $FCRL5^+$ B cells exhibit expression patterns comparable to human atMBCs for a substantial number of immune- related genes, perhaps most notably the master transcription factor T-bet. Mouse $FCRL5^+$ B cells also share markers with ABCs, which resemble atMBCs (Rubtsova et al., 2015). Another research group recently reached similar conclusions after analyzing MSP1-specific BCR-transgenic B cells in an adoptive transfer model of *P. chabaudi* infection (Pérez-Mazliah et al., 2018); our study complements theirs by characterizing the poly-clonal responses of endogenous B cells to the same pathogen.

An additional conclusion that emerges from our data is that cells with an atypical phenotype are probably a heterogeneous population. We have shown that whereas primary plasmablasts express little to no FCRL5, plasmablasts arising early in the secondary response do, likely because they are derived from $FCRL5^+$ MBCs. Atypical markers are robustly expressed on

MBCs during infection (28 d.p.i.) and remain elevated, although modestly, on long-lived FCRL5$^+$ MBCs well after infection is cleared (150 d.p.i.) Thus, depending on context, B cells expressing atypical markers may include secondary plasmablasts, recently activated B cells, and both quiescent and activated MBCs; further markers must be used to distinguish between these populations. In human studies, expression levels of CD11c and other atypical markers vary greatly on atMBCs from individual subjects, reinforcing the hypothesis that this is a heterogenous population whose composition and marker expression levels reflect time since antigen exposure (Weiss et al., 2009; Sullivan et al., 2015).

We have found that in *Plasmodium*-infected mice, FCRL5$^+$ B cells comprise the majority of long-lived SwIg MBCs and that they respond to challenge as well as or better than FCRL5$^-$B cells, upregulating additional atypical markers as they do so. In light of these data, we have revisited previous reports of atMBC function in humans. One previous study concluded that atMBCs contributed as much as cMBCs to serum antibody levels. Furthermore, atMBCs but not cMBCs expressed the proliferation marker Ki67 when examined directly *ex vivo*, suggesting recent activation (Muellenbeck et al., 2013). However, other studies, which exam- ined atMBCs and cMBCs following *ex vivo* restimulation, found that atMBCs from chronically exposed patients gave rise to fewer antibody-secreting cells than cMBCs and exhibited diminished BCR signaling and poor proliferation (Obeng-Adjei et al., 2017; Portugal et al., 2015; Sullivan et al., 2015).

How can these apparently conflicting results be reconciled? The first study examined antibody production from serum, whereas the latter two measured it on restimulated cells. If many atMBCs are recently activated MBCs, as our evidence suggests, then it makes sense that they would contribute to serum antibody and express Ki67 when analyzed directly *ex vivo* but might be refractory to further activation upon restimulation. In support of this hypothesis, we note that two studies reporting diminished induction of BCR signaling in atMBCs do not actually demonstrate that atMBCs have lower activation after restimulation but rather exhibit markedly higher baseline activation compared to cMBCs (Obeng-Adjei et al., 2017; Portugal et al., 2015). It is also possible that conditions in some restimulation as- says were not optimal for eliciting antibody secretion from atMBCs: for example, atMBC-like cells isolated from human tonsils will respond more robustly than cMBCs when treated with cytokines and CD40L but not with a BCR crosslinking antibody (Ehrhardt et al., 2005). Similarly, ABCs respond well to BCR stimulation only in the presence of a TLR ligand (Rubtsova et al., 2015), whereas CD27$^-$FCRL5$^+$ B cells from humans with lupus efficiently differentiate into plasmablasts and secrete autoantibody when co-cultured with activated T cells *ex vivo* (Wang et al., 2018). Finally, different studies have analyzed PBMCs taken from human subjects of different ages, and the infection and/or exposure status of each subject is not always clear. Thus, differences in the developmental stage or activation state of B cells at the time of sampling may underlie some of the variation in human studies.

We have also shown that human CD21$^+$ CD27$^+$ MBCs specific for TTCF, a component of the tetanus vaccine, express significant levels of FCRL5 and CD11c. This expression pattern was not observed in bulk (non-antigen-specific) CD21$^+$ CD27$^+$ MBCs but could be revealed by enriching for rare antigen-specific cells. These TTCF-specific MBCs were likely all elicited in the presence of aluminum-based vaccine adjuvants, which efficiently recruit T

cell help to generate GC-derived MBCs (Kool et al., 2012). In contrast, the bulk memory population likely includes MBCs that developed under a range of conditions, with varying levels of T cell help and GC participation. Thus, we suggest that in humans, "atypical" markers actually denote high-quality MBCs that were generated through T cell and GC interactions. These make up a minority fraction of the total $CD21^+$ $CD27^+$ pool but are significantly enriched among vac- cine-elicited MBCs. This hypothesis is consistent with data from our mouse model showing ubiquitous expression of FCRL5 on $CD73^+$ $CD80^+$ MBCs. It should further be noted that although FCRL5 expression is more prevalent on human atMBCs, 5%–45% of bulk human cMBCs also express FCRL5 (Figure 7I; Sullivan et al., 2015). We suggest that atypical markers are enriched in the bulk $CD21^-CD27^-$subset of human B cells because this population represents MBCs that have recently been reactivated (Agematsu et al., 1997; Masilamani et al., 2003); therefore, it is enriched for long-lived, GC-derived, optimally responsive B cells that quickly activate following secondary antigen exposure.

One important difference between our study and most published work on human atMBCs is that here, the mouse $FCRL5^+$ subset was examined in the context of a single infection and challenge, whereas most human studies assess patients after many repeated infections. Although *P. chabaudi* is considered a chronic model, with parasites persisting up to 3 months, it is possible that it does not adequately replicate the chronic conditions of repeated human exposure to *Plasmodium*, which may alter the functional capacity of atMBCs. Further studies in persistently infected mice (Fontana et al., 2016) are planned to address this critical issue. Interestingly, atMBCs from HIV viremic patients produced more HIV-specific antibodies than cMBCs (Moir et al., 2008), suggesting that these cells can retain secre- tory capacity despite chronic antigen exposure. Moreover, higher atMBC frequencies are associated with clinical immunity to malaria, perhaps pointing to a protective role for these cells (Sullivan et al., 2016). It is to be hoped that by improving our understanding of the B cell populations that arise during *Plasmodium* infection, their role in protection, and the signals that coordinate their development and retention, we may gain important insights into rational vaccine designs and therapeutic interventions that will permit protective B cell responses to develop in humans.

STAR★METHODS

CONTACT FOR REAGENT AND RESOURCE SHARING

Further information and requests for resources and reagents should be directed to and will be fulfilled by the Lead Contact, Mary Fontana (mfontana@uw.edu).

EXPERIMENTAL MODEL AND SUBJECT DETAILS

Mice—Mice were group-housed on a twelve-hour light-dark cycle under specific pathogen-free conditions. Experiments were conducted at both the University of Washington and UCSF, and similar results were obtained in both locations. 8–12 week old male and female mice were used for all experiments, with the exception of LCMV infections, which were initiated in 5–6 week old mice. Mice were age- and sex-matched within each experiment. Wild-type C57BL/6J (B6) mice were from Jackson Laboratories or the National Cancer

Institute. CD45.1$^+$, *Ifngr1*$^{-/-}$ and *Tbx21*$^{fl/fl}$ mice were from Jackson Laboratories. *Tbx21*$^{fl/fl}$ mice were crossed in-house to *Mb1-Cre* mice (M. Reth, Max Planck Institute of Immunobiology and Epigenetics), and CD45.1$^+$ mice were crossed to B6 (CD45.2$^+$) mice. All mouse experiments were conducted with the approval of the UCSF or UW Institutional Animal Care and Use Committees in accordance with the guidelines of the NIH Office of Laboratory Animal Welfare.

Infectious agents—*Plasmodium chabaudi* AS and *P. yoelii* 17XNL were obtained from the MR4 Stock center and passaged in B6 mice. LCMV Armstrong was obtained from M. Bevan (University of Washington).

Human PBMCs—De-identified PBMCs from 8 American donors were purchased from Bloodworks Northwest Blood Bank (Seattle, WA), either as frozen PBMCs or in Leukocyte Reduction System (LRS) filters, or were gifted from D. Rawlings (Seattle Children's Research Institute). PBMCs from D. Rawlings were collected with approval from the Fred Hutchinson Cancer Research Center Institutional Review Board (Protocol FH985.03), and all donors gave informed consent. PBMCs from LRS filters were isolated over Ficoll gradients and frozen before thawing for analysis. No identifying information was available for LRS filters (n = 3) due to blood center protocols for collection and processing. Remaining donors were 3 males and 2 females between 28 and 40 years old. For donors yielding sufficient cell numbers, 2–3 technical replicates were performed and averaged to generate the values graphed in Figure 7.

METHOD DETAILS

Infections and immunizations

For *Plasmodium* infections, mice were injected intraperitoneally (i.p.) with 10^6 infected RBCs. Parasitemia was monitored by thin blood smear stained with Giemsa (Huang et al., 2015). Challenge experiments were performed with 10^7 infected RBCs administered i.p. and were analyzed 3 or 5 d after challenge, as specified. For LCMV infections, 2×10^5 pfu of LCMV Armstrong were injected i.p. into 5–6 week old mice. For protein immunizations, 50 μg ovalbumin (OVA; Sigma) in PBS was diluted 1:1 in Imject alum (Pierce) and administered i.p. Mice were randomly assigned to experimental groups.

Adoptive transfer

5 million CD45.1$^+$/CD45.2$^+$ splenic follicular B cells (FCRL5$^-$ CD21^{lo} CD23^{hi} CD138$^-$ GL7$^-$) from naive mice were sorted on a FACSAria (BD) and injected retro-orbitally into CD45.2$^+$ B6 recipients, some of which were infected with *P. chabaudi* 1 d after cell transfer.

Flow cytometry

Blood was obtained from the submandibular vein or by cardiac puncture following euthanasia. Spleens were excised from euthanized animals, manually disrupted, and passed through nylon mesh to obtain single-cell suspensions. Peritoneal cells were obtained by lavage with 8 mL PBS following euthanasia. RBCs were lysed in ACK buffer and samples were blocked with α-CD16/CD32 prior to labeling with antibodies. To analyze antigen-

specific cells, splenocytes were incubated first with a decoy reagent labeled in-house with APC-Dylight755 (for APC-conjugated tetramers) or PE-AlexaFluor647 (for PE tetramers), then with fluorescently labeled tetramer. Tetramers were made by biotinylating and conjugating the following proteins to streptavidin-APC or -PE: MSP1–19 and Tetanus Toxoid C Fragment (both expressed in-house), OVA (Sigma), and LCMV Glycoprotein (kind gift of J. Teijaro). Magnetic anti-APC or anti-PE beads were used to enrich tetramer-positive cells after labeling (Krishnamurty et al., 2016; Taylor et al., 2012). For intracellular labeling, cells were fixed and permeabilized with the Transcription Factor Staining Buffer Set (eBioscience) and incubated with antibodies overnight. Data were collected on an LSRII (BD) or Aurora (Cytek) and analyzed using FlowJo software (Treestar). For human samples, 6–10 × 10^7 PBMCs were thawed, labeled with TTCF tetramer as for mouse samples, and fixed in 4% paraformaldehyde before analyzing on an LSRII. Antibodies are listed in the Key Resources Table.

RNA-Seq

Class-switched B cells ($CD19^+$ $CD138^-$ IgM^- IgD^-) were double-sorted on a FACSAria into highly purified $FCRL5^+$ and $FCRL5^-$ populations from the blood of *Ifngr1*$^{-/-}$mice 21 d.p.i. with *P. chabaudi*. One hundred cells were sorted directly into lysis buffer, and RNA was isolated with the RNAqeous Micro Kit (Life Technologies). Sequencing libraries were prepared using a modified SMART-Seq2 protocol (Picelli et al., 2014), skipping the lysis procedure. Multiplexed libraries were sequenced as 50 nt single end reads on a HiSeq 2500 in high output mode. Reads were aligned using RSEM 1.2.22 and STAR 2.4.2a to GRCm38. Samples with fewer than 1 million aligned reads or < 50% of reads aligning were excluded from further processing. Reliably detected transcripts were determined by discounting genes classified by DESeq2 as questionably or not expressed. For differential gene expression analysis, DESeq2 was used to identify significantly differentially expressed genes between $FCRL5^+$ and $FCRL5^-$ cells (adjusted $p < 5\%$). All RNA-Seq data are available in the Gene Expression Omnibus (https://www.ncbi.nlm.nih.gov/geo) at GEO: GSE85205. Functional enrichment analysis was performed on differentially expressed genes using DAVID (Dennis et al., 2003).

Bioinformatic comparison of human and mouse transcriptional data

Genes differentially expressed by cMBCs and atMBCs from human subjects exposed to *P. falciparum* were obtained from Table S1 of Sullivan et al. (2015). Human gene symbols were converted to mouse symbols using the Mouse Genome Informatics “Mouse/Hu- man Orthology with Phenotype Annotations” conversion table. The intersection of human MBC subset-distinguishing genes with mouse FCRL5 subset-distinguishing genes was identified and visualized as a heatmap using custom scripts. To test significance, we first restricted our analysis to genes that were represented in both the mouse and human dataset. We then used two independent online tools (links in Key Resources Table) to calculate a hypergeometric probability using the following values: successes of sample x (genes that were DE in the same direction in both human and mouse) = 34; sample size n (mouse DE genes) = 232; successes of lot M (DE genes in human) = 1066; lot size N (all genes present in both mouse and human datasets) = 15592. Similar p values were obtained from both calculators.

EliSPOT

EliSPOT assays were performed on MSP1-specific memory B cells ($B220^+$ $CD138^-$ $CD38^+$ $GL7^-$ IgD^-; FCRL5 expression as indicated) sorted from spleens harvested 3–4 months post-infection with *P. chabaudi*. 1000–5000 MBCs per well were plated along with 50,000 non-B cells sorted in parallel from the same samples. Cells were incubated for 3 d with IL-2 (10 μg/mL) and R848 (1 μg/mL). After incubation, plates were washed and total ASCs were detected with biotinylated IgM (II/41) and pan-IgG (poly4053) antibodies. Plates were imaged on a CTL EliSPOT reader and spots were counted using ImageJ software. The number of spots was normalized to the total number of MBCs plated per well. Technical triplicates were performed for each independent experiment.

QUANTIFICATION AND STATISTICAL ANALYSIS

All statistics were calculated using Prism 7 software. Non-parametric tests were used to analyze data from *in vivo* studies. Paired tests were used when the values being compared derived from the same sample (e.g., $FCRL5^+$ and $FCRL5^-$ populations from a single mouse); otherwise, unpaired tests were performed. The statistical tests used are listed in each figure legend.

DATA AND SOFTWARE AVAILABILITY

RNA-seq data can be found at GEO: GSE85205.

Supplementary Material

Refer to Web version on PubMed Central for supplementary material.

ACKNOWLEDGMENTS

We thank B. Greenhouse, R. Sullivan, and members of the Pepper lab for helpful discussions; J. Rivera for technical assistance; M. Reth for *Mb1-Cre* mice; D. Rawlings for human PBMCs; and J. Teijaro for the LCMV glycoprotein. This work was supported by NIAID T32 grant AI007334 and NIAID R21 AI139740 to M.F.F. and NIAID R00 AI085035, NIAID R21 AI114916, and a UCSF Program for Breakthrough Biomedical Research award to C.C.K. The funders played no role in study design, data collection and interpretation, or decision to publish. All data are included in this manuscript, supplementary figures, or at GEO: GSE85205.

REFERENCES

Agematsu K, Nagumo H, Yang FC, Nakazawa T, Fukushima K, Ito S, Sugita K, Mori T, Kobata T, Morimoto C, and Komiyama A (1997). B cell subpopulations separated by CD27 and crucial collaboration of CD27+ B cells and helper T cells in immunoglobulin production. Eur. J. Immunol 27, 2073–2079. [PubMed: 9295047]

Charles ED, Brunetti C, Marukian S, Ritola KD, Talal AH, Marks K, Jacobson IM, Rice CM, and Dustin LB (2011). Clonal B cells in patients with hepatitis C virus-associated mixed cryoglobulinemia contain an expanded anergic CD21low B-cell subset. Blood 117, 5425–5437. [PubMed: 21421840]

Choi YS, and Baumgarth N (2008). Dual role for B-1a cells in immunity to influenza virus infection. J. Exp. Med 205, 3053–3064. [PubMed: 19075288]

Davis RS (2015). FCRL regulation in innate-like B cells. Ann. NY Acad. Sci 1362, 110–116. [PubMed: 25964091]

Dennis G Jr., Sherman BT, Hosack DA, Yang J, Gao W, Lane HC, and Lempicki RA (2003). DAVID: Database for Annotation, Visualization, and Integrated Discovery. Genome Biol 4, 3.

Dobin A, Davis CA, Schlesinger F, Drenkow J, Zaleski C, Jha S, Batut P, Chaisson M, and Gingeras TR (2013). STAR: ultrafast universal RNA-seq aligner. Bioinformatics 29, 15–21. [PubMed: 23104886]

Ehrhardt GRA, Hsu JT, Gartland L, Leu C-M, Zhang S, Davis RS, and Cooper MD (2005). Expression of the immunoregulatory molecule FcRH4 defines a distinctive tissue-based population of memory B cells. J. Exp. Med 202, 783–791. [PubMed: 16157685]

Fontana MF, Baccarella A, Craft JF, Boyle MJ, McIntyre TI, Wood MD, Thorn KS, Anidi C, Bayat A, Chung MR, et al. (2016). A Novel Model of Asymptomatic Plasmodium Parasitemia That Recapitulates Elements of the Human Immune Response to Chronic Infection. PLoS One 11, e0162132. [PubMed: 27583554]

Franco A, Kraus Z, Li H, Seibert N, Dement-Brown J, and Tolnay M (2018). CD21 and FCRL5 form a receptor complex with robust B-cell activating capacity. Int. Immunol 30, 569–578. [PubMed: 30107486]

Haas KM, Poe JC, Steeber DA, and Tedder TF (2005). B-1a and B-1b cells exhibit distinct developmental requirements and have unique functional roles in innate and adaptive immunity to S. pneumoniae. Immunity 23, 7–18. [PubMed: 16039575]

Hao Y, O'Neill P, Naradikian MS, Scholz JL, and Cancro MP (2011). A B-cell subset uniquely responsive to innate stimuli accumulates in aged mice. Blood 118, 1294–1304. [PubMed: 21562046]

Harms Pritchard G, and Pepper M (2018). Memory B cell heterogeneity: Remembrance of things past. J. Leukoc. Biol 103, 269–274. [PubMed: 29345369]

Hayakawa K, Ishii R, Yamasaki K, Kishimoto T, and Hardy RR (1987). Isolation of high-affinity memory B cells: phycoerythrin as a probe for anti- gen-binding cells. Proc. Natl. Acad. Sci. USA 84, 1379–1383. [PubMed: 3493491]

Huang BW, Pearman E, and Kim CC (2015). Mouse Models of Uncomplicated and Fatal Malaria. Biol. Protoc 5, e1514.

Jacobi AM, Reiter K, Mackay M, Aranow C, Hiepe F, Radbruch A, Hansen A, Burmester G-R, Diamond B, Lipsky PE, and Dörner T (2008). Activated memory B cell subsets correlate with disease activity in systemic lupus erythematosus: delineation by expression of CD27, IgD, and CD95. Arthritis Rheum 58, 1762–1773. [PubMed: 18512812]

Jones DD, Wilmore JR, and Allman D (2015). Cellular dynamics of memory B cell populations: IgM+ and IgG+ memory B cells persist indefinitely as quiescent cells. J. Immunol 195, 4753–4759. [PubMed: 26438523]

Kool M, Fierens K, and Lambrecht BN (2012). Alum adjuvant: some of the tricks of the oldest adjuvant. J. Med. Microbiol 61, 927–934. [PubMed: 22174375]

Krishnamurty AT, Thouvenel CD, Portugal S, Keitany GJ, Kim KS, Holder A, Crompton PD, Rawlings DJ, and Pepper M (2016). Somatically Hypermutated Plasmodium-Specific IgM(+) Memory B Cells Are Rapid, Plas- tic, Early Responders upon Malaria Rechallenge. Immunity 45, 402–414. [PubMed: 27473412]

Li B, and Dewey CN (2011). RSEM: accurate transcript quantification from RNA-Seq data with or without a reference genome. BMC Bioinformatics 12, 323. [PubMed: 21816040]

Li FJ, Won WJ, Becker EJ Jr., Easlick JL, Tabengwa EM, Li R, Shakhmatov M, Honjo K, Burrows PD, and Davis RS (2014). Emerging roles for the FCRL family members in lymphocyte biology and disease. Curr. Top. Microbiol. Immunol 382, 29–50. [PubMed: 25116094]

Love MI, Huber W, and Anders S (2014). Moderated estimation of fold change and dispersion for RNA-seq data with DESeq2. Genome Biol 15, 550. [PubMed: 25516281]

Masilamani M, Kassahn D, Mikkat S, Glocker MO, and Illges H (2003). B cell activation leads to shedding of complement receptor type II (CR2/CD21). Eur. J. Immunol 33, 2391–2397 [PubMed: 12938215]

Moir S, and Fauci AS (2014). B-cell exhaustion in HIV infection: the role of immune activation. Curr. Opin. HIV AIDS 9, 472–477. [PubMed: 25023621]

Moir S, Ho J, Malaspina A, Wang W, DiPoto AC, O'Shea MA, Roby G, Kottilil S, Arthos J, Proschan MA, et al. (2008). Evidence for HIV-asso- ciated B cell exhaustion in a dysfunctional memory B cell compartment in HIV- infected viremic individuals. J. Exp. Med 205, 1797–1805. [PubMed: 18625747]

Muellenbeck MF, Ueberheide B, Amulic B, Epp A, Fenyo D, Busse CE, Esen M, Theisen M, Mordmüller B, and Wardemann H (2013). Atypical and classical memory B cells produce Plasmodium falciparum neutralizing antibodies. J. Exp. Med 210, 389–399. [PubMed: 23319701]

Obeng-Adjei N, Portugal S, Holla P, Li S, Sohn H, Ambegaonkar A, Skinner J, Bowyer G, Doumbo OK, Traore B, et al. (2017). Malariainduced interferon-γ drives the expansion of Tbethi atypical memory B cells. PLoS Pathog. 13, e1006576. [PubMed: 28953967]

Pérez-Mazliah D, Gardner PJ, Schweighoffer E, McLaughlin S, Hosking C, Tumwine I, Davis RS, Potocnik AJ, Tybulewicz VL, and Langhorne J (2018). Plasmodium-specific atypical memory B cells are short-lived activated B cells. eLife 7, e39800. [PubMed: 30387712]

Picelli S, Faridani OR, Björklund ÅK, Winberg G, Sagasser S, and Sandberg R (2014). Full-length RNA-seq from single cells using Smart- seq2. Nat. Protoc 9, 171–181. [PubMed: 24385147]

Portugal S, Pierce SK, and Crompton PD (2013). Young lives lost as B cells falter: what we are learning about antibody responses in malaria. J. Immunol 190, 3039–3046. [PubMed: 23526829]

Portugal S, Tipton CM, Sohn H, Kone Y, Wang J, Li S, Skinner J, Virtaneva K, Sturdevant DE, Porcella SF, et al. (2015). Malaria-associated atypical memory B cells exhibit markedly reduced B cell receptor signaling and effector function. eLife 4, e07218.

Rakhmanov M, Keller B, Gutenberger S, Foerster C, Hoenig M, Driessen G, van der Burg M, van Dongen JJ, Wiech E, Visentini M, et al. (2009). Circulating CD21low B cells in common variable immunodeficiency resemble tissue homing, innate-like B cells. Proc. Natl. Acad. Sci. USA 106, 13451–13456. [PubMed: 19666505]

Roark JH, Park SH, Jayawardena J, Kavita U, Shannon M, and Bendelac A (1998). CD1.1 expression by mouse antigen-presenting cells and marginal zone B cells. J. Immunol 160, 3121–3127. [PubMed: 9531266]

Rubtsov AV, Rubtsova K, Fischer A, Meehan RT, Gillis JZ, Kappler JW, and Marrack P (2011). Toll-like receptor 7 (TLR7)-driven accumulation of a novel CD11c^{+} B-cell population is important for the development of auto- immunity. Blood 118, 1305–1315. [PubMed: 21543762]

Rubtsova K, Rubtsov AV, van Dyk LF, Kappler JW, and Marrack P (2013). T-box transcription factor T-bet, a key player in a unique type of B-cell activation essential for effective viral clearance. Proc. Natl. Acad. Sci. USA 110, E3216–E3224. [PubMed: 23922396]

Rubtsova K, Rubtsov AV, Cancro MP, and Marrack P (2015). Age-Associated B Cells: A T-bet-Dependent Effector with Roles in Protective and Pathogenic Immunity. J. Immunol 195, 1933–1937. [PubMed: 26297793]

Ryg-Cornejo V, Ly A, and Hansen DS (2016). Immunological processes underlying the slow acquisition of humoral immunity to malaria. Parasitology 143, 199–207. [PubMed: 26743747]

Schofield L, and Mueller I (2006). Clinical immunity to malaria. Curr. Mol. Med 6, 205–221. [PubMed: 16515511]

Scholzen A, Teirlinck AC, Bijker EM, Roestenberg M, Hermsen CC, Hoffman SL, and Sauerwein RW (2014). BAFF and BAFF receptor levels correlate with B cell subset activation and redistribution in controlled human malaria infection. J. Immunol 192, 3719–3729. [PubMed: 24646735]

Speiser DE, Utzschneider DT, Oberle SG, Munz €C, Romero P, and Zehn D (2014). T cell differentiation in chronic infection and cancer: functional adaptation or exhaustion? Nat. Rev. Immunol 14, 768–774. [PubMed: 25257362]

Stephens R, Culleton RL, and Lamb TJ (2012). The contribution of Plasmodium chabaudi to our understanding of malaria. Trends Parasitol 28, 73–82. [PubMed: 22100995]

Sullivan RT, Kim CC, Fontana MF, Feeney ME, Jagannathan P, Boyle MJ, Drakeley CJ, Ssewanyana I, Nankya F, Mayanja-Kizza H, et al. (2015). FCRL5 Delineates Functionally Impaired Memory B Cells Associated with Plasmodium falciparum Exposure. PLoS Pathog 11, e1004894. [PubMed: 25993340]

Sullivan RT, Ssewanyana I, Wamala S, Nankya F, Jagannathan P, Tappero JW, Mayanja-Kizza H, Muhindo MK, Arinaitwe E, Kamya M, et al. (2016). B cell sub-types following acute malaria and associations with clinical immunity. Malar. J 15, 139. [PubMed: 26939776]

Taylor JJ, Pape KA, and Jenkins MK (2012). A germinal center-independent pathway generates unswitched memory B cells early in the primary response. J. Exp. Med 209, 597–606. [PubMed: 22370719]

Tomayko MM, Steinel NC, Anderson SM, and Shlomchik MJ (2010). Cutting edge: Hierarchy of maturity of murine memory B cell subsets. J. Immunol 185, 7146–7150. [PubMed: 21078902]

Waffarn EE, Hastey CJ, Dixit N, Soo Choi Y, Cherry S, Kalinke U, Simon SI, and Baumgarth N (2015). Infection-induced type I interferons activate CD11b on B-1 cells for subsequent lymph node accumulation. Nat. Commun 6, 8991. [PubMed: 26612263]

Wang S, Wang J, Kumar V, Karnell JL, Naiman B, Gross PS, Rahman S, Zerrouki K, Hanna R, Morehouse C, et al.; Autoimmunity Molecular Medicine Team (2018). IL-21 drives expansion and plasma cell differentiation of autoreactive CD11c^{hi}T-bet^{+} B cells in SLE. Nat. Commun 9, 1758. [PubMed: 29717110]

Weiss GE, Crompton PD, Li S, Walsh LA, Moir S, Traore B, Kayentao K, Ongoiba A, Doumbo OK, and Pierce SK (2009). Atypical memory B cells are greatly expanded in individuals living in a malaria-endemic area. J. Immunol 183, 2176–2182. [PubMed: 19592645]

Wherry EJ, and Kurachi M (2015). Molecular and cellular insights into T cell exhaustion. Nat. Rev. Immunol 15, 486–499. [PubMed: 26205583]

Wherry EJ, Ha S-J, Kaech SM, Haining WN, Sarkar S, Kalia V, Subramaniam S, Blattman JN, Barber DL, and Ahmed R (2007). Molecular signature of CD8+ T cell exhaustion during chronic viral infection. Immunity 27, 670–684. [PubMed: 17950003]

Zheng-Bradley X, Rung J, Parkinson H, and Brazma A (2010). Large scale comparison of global gene expression patterns in human and mouse. Genome Biol 11, R124. [PubMed: 21182765]

Zhu Z, Li R, Li H, Zhou T, and Davis RS (2013). FCRL5 exerts binary and compartment-specific influence on innate-like B-cell receptor signaling. Proc. Natl. Acad. Sci. USA 110, E1282–E1290. [PubMed: 23509253]

Zuccarino-Catania GV, Sadanand S, Weisel FJ, Tomayko MM, Meng H, Kleinstein SH, Good-Jacobson KL, and Shlomchik MJ (2014). CD80 and PD-L2 define functionally distinct memory B cell subsets that are independent of antibody isotype. Nat. Immunol 15, 631–637. [PubMed: 24880458]

Highlights

- Antigen-specific FCRL5^{+} memory B cells (MBCs) expand in Plasmodium-infected mice
- Murine FCRL5^{+} MBCs resemble human atypical MBCs from Plasmodium-exposed humans
- FCRL5^{+} MBCs are mature, long-lived, and respond robustly to *in vivo* challenge
- Antigen-specific FCRL5^{+} MBCs are generated by immunization in both mice and humans

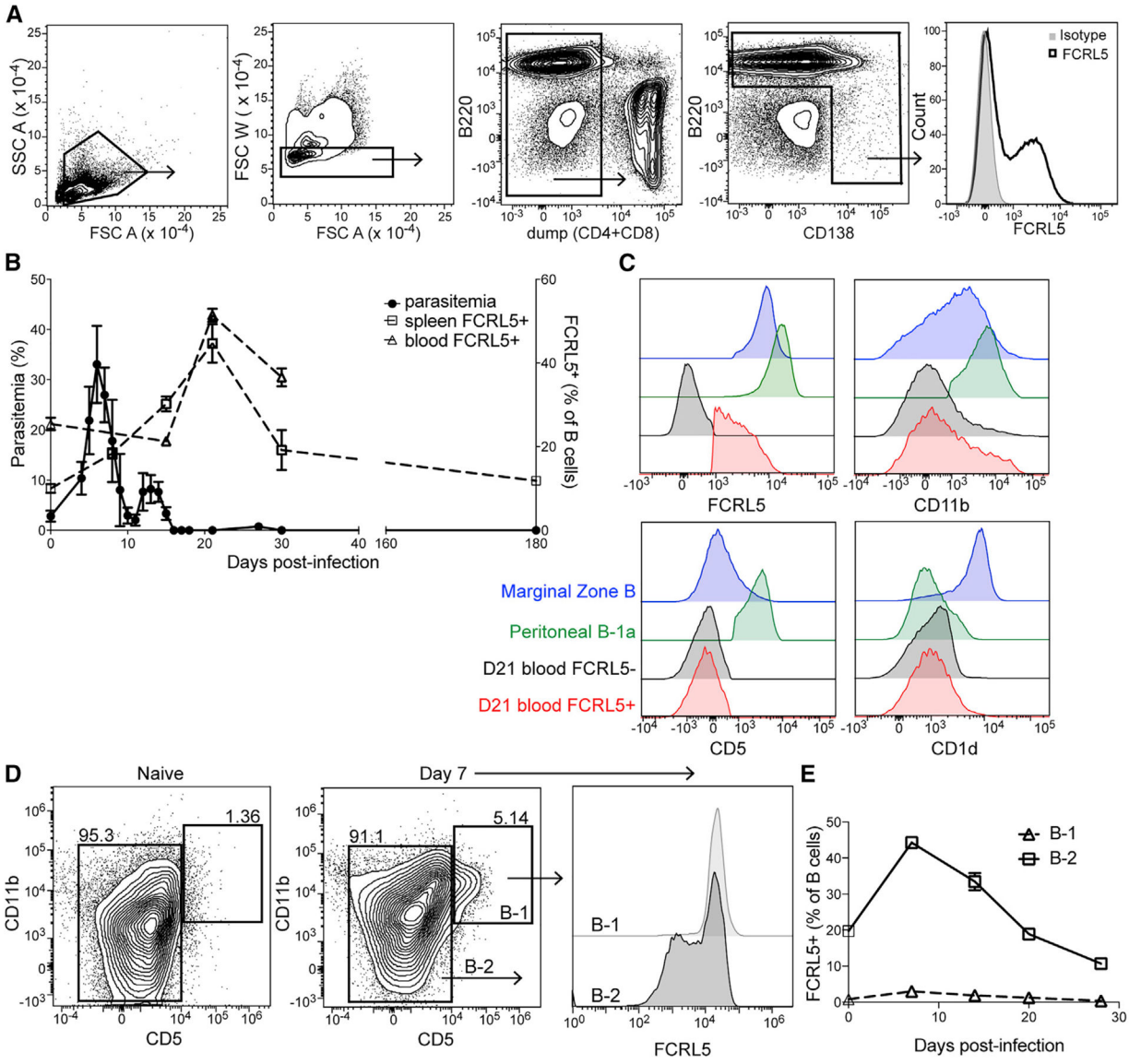

Figure 1. Infection with *P. chabaudi* Elicits Expansion of FCRL5^{+} B Cells

Wild-type (B6) mice were infected with *P. chabaudi* AS.

(A) Gating strategy for assessing FCRL5 expression on B cells. A representative blood sample from an infected mouse is shown.

(B) Parasitemia (% of red blood cells infected; solid line) and frequencies of FCRL5^{+} B cells in the blood and spleen (dashed lines) were assessed over time.

(C) Indicated markers were assessed by flow cytometry on marginal zone B and peritoneal B-1a cells from naive mice, or FCRL5^{+} or FCRL5^{-}B cells from the blood of mice infected for 21 days. Representative plots are shown (n = 4).

(D) Representative plots depicting FCRL5 expression on B-1a (CD11b^{hi} CD5^{+}) and B-2 (CD11b$^{lo/-}$CD5^{-}) cells in the blood of naive and infected mice.

(E) Frequency of FCRL5^{+} B-1a and B-2 cells after infection. Time course graphs depict mean ± SEM of 5 mice from one representative experiment, out of 3.

See also Figure S1.

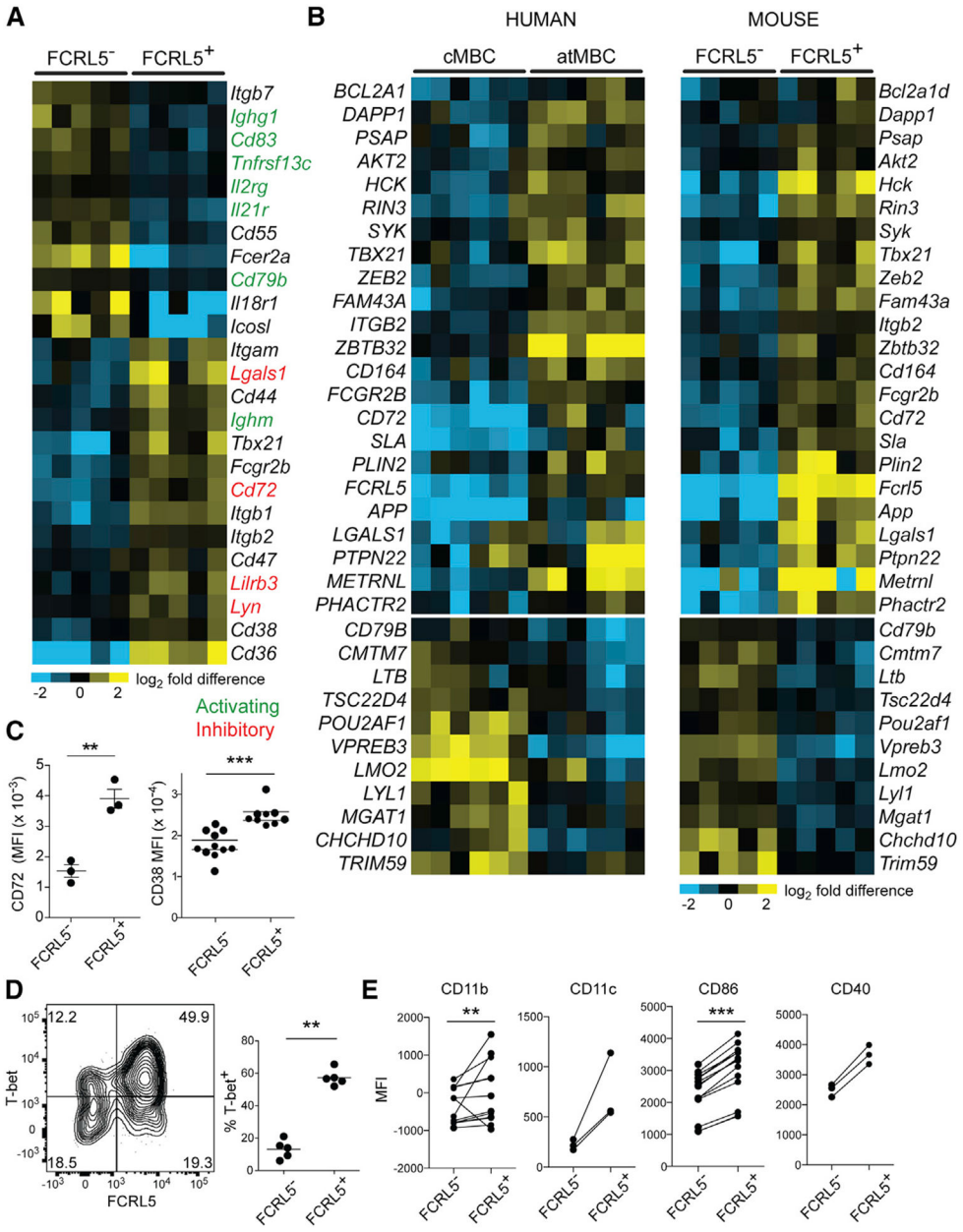

Figure 2. Similarities between Infection-Induced Mouse FCRL5$^+$ B Cells and atMBCs from *Plasmodium*-Infected Humans

(A) RNA-seq was performed on class-switched (IgM$^-$IgD$^-$), FCRL5$^-$or FCRL5$^+$ B cells sorted from the blood of *Ifngr1*$^{-/-}$mice infected for 21 days with *P. chabaudi*. Columns represent individual mice (n = 5). Select genes involved in immune signaling are shown. Genes with putative activating function are labeled in green; those with putative inhibitory function are labeled in red.

(B) Heatmaps depict all genes that are differentially regulated in both human atMBCs (left) and mouse FCRL5$^+$ B cells, relative to cMBCs and FCRL5$^-$B cells, respectively. Human data are from Sullivan et al. (2015).

(C–E) Expression of (C) CD72 and CD38, (D) T-bet, and (E) CD11b, CD11c, CD86, and CD40 were measured by flow cytometry in blood B cells 21 d.p.i.
**$p < 0.01$; ***$p < 0.001$ by paired t test (Wilcoxon rank-sum test). See also Figure S2 and Tables S1 and S2.

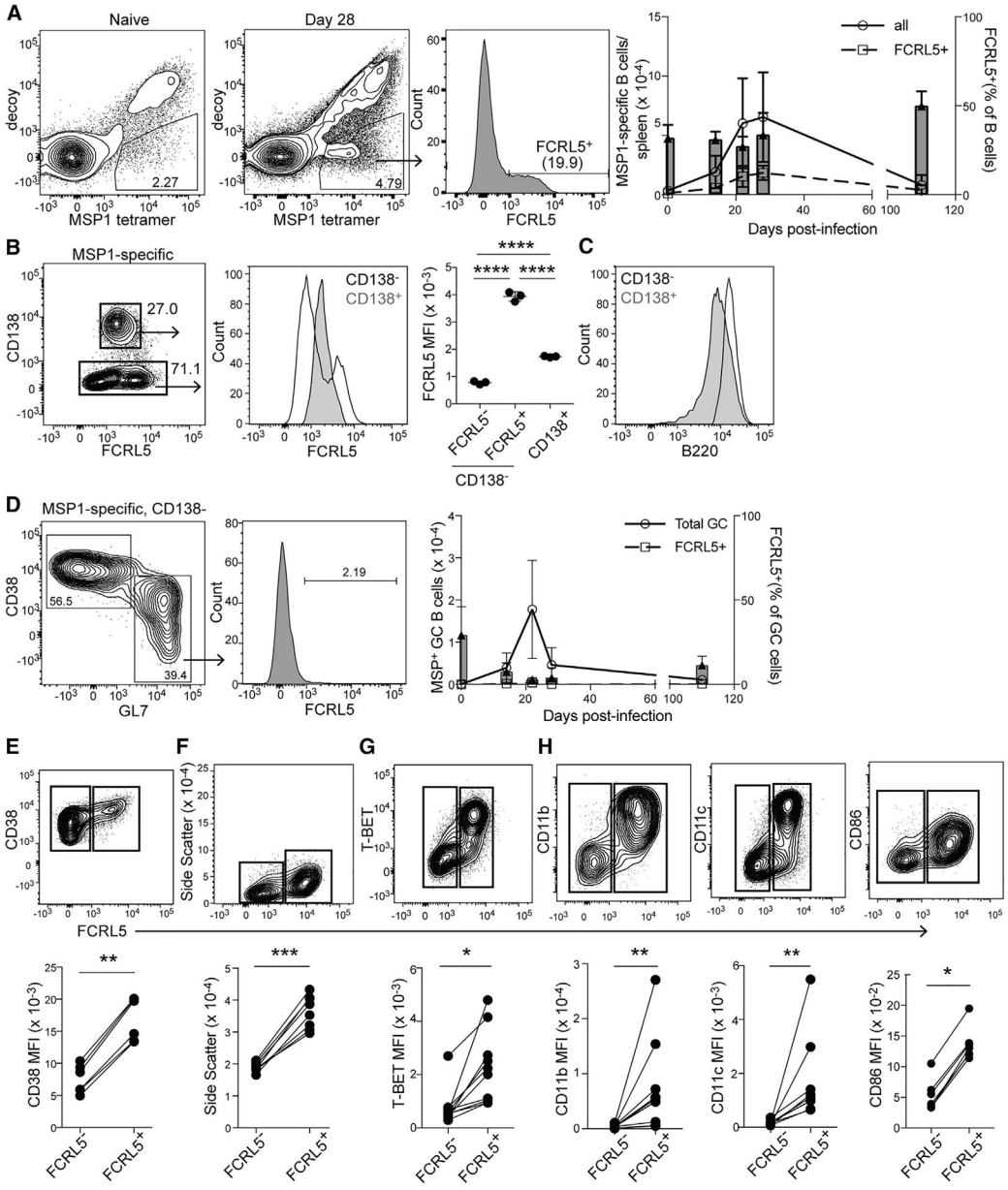

Figure 3. FCRL5 Is Expressed on Antigen-Specific MBCs

Mice were infected with *P. chabaudi*, and splenic B cells specific for the *P. chabaudi* antigen MSP1 were labeled with tetramer, magnetically enriched, and analyzed by flow cytometry. In time course graphs, mean ± SEM is depicted; gray bars indicate percentage of MSP1-specific cells that express FCRL5 at each time point.

(A) Gating and quantification of FCRL5$^+$ and total MSP1-specific B cells.

(B) FCRL5 expression on MSP1-specific CD138$^+$ plasma cells 28 d.p.i.

(C) B220 expression on the CD138$^+$ and CD138$^-$populations from (B).

(D) Gating and quantification of MSP1-specific GC B cells following infection.

(E–H) Levels of (E) CD38, (F) side scatter, (G) T-bet, and (H) indicated atypical markers in memory-naive MSP1-specific B cells (B220$^+$ CD38$^+$ CD138$^-$GL7$^-$) gated by FCRL5

expression as indicated. All plots depict data gathered 28 d.p.i. except (G) (21 d.p.i.) and (H) (graphs pooled from between 21 and 40 d.p.i.). Results are pooled from two independent experiments with at least 3 mice per time point per experiment. (E–H) Each dot represents one mouse. *$p < 0.05$; **$p < 0.01$; ***$p < 0.001$ by paired t test (Wilcoxon rank-sum test). ****$p < 0.0001$ by one-way ANOVA with Tukey's post-test.

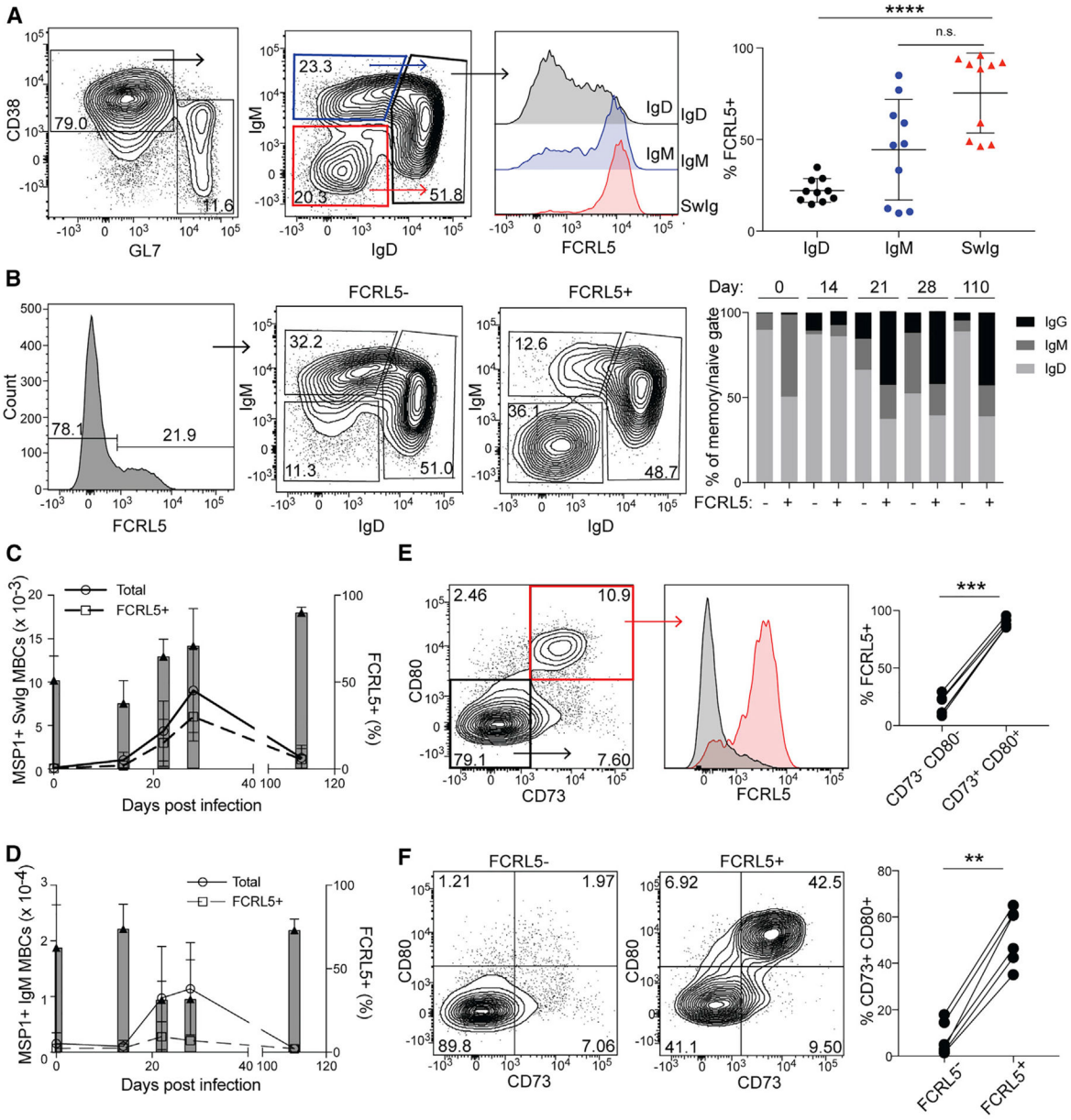

Figure 4. FCRL5^{+} MBCs Are Enriched for Class-Switching and Expression of Memory Markers

Splenic MSP1-specific B cells with a memory-naive phenotype (B220^{+} CD38^{+} CD138^{-}GL7^{-}) were examined 28 d.p.i. (flow plots) or at indicated time points (time courses).

(A) Gating (left) and quantification (right) of FCRL5 expression on cells expressing IgD or IgM or neither (SwIg).

(B) The memory-naive gate was first divided into FCRL5^{+} and FCRL5^{-}populations and then examined for isotype distribution.

(C) Quantification of SwIg and (D) IgM^{+}, total and FCRL5^{+} memory-naive cells following infection. Grey bars indicate % FCRL5^{+} at each time point.

(E) FCRL5 expression on CD73^{+} CD80^{+} cells versus double-negative cells.

(F) The memory-naive gate was first divided into FCRL5^{+} and FCRL5^{-}populations and then examined for CD73 and CD80 expression.

**p < 0.01; ***p < 0.001 by paired t test (Wilcoxon rank-sum test). ****p < 0.0001 by one-way ANOVA with Tukey's post-test. See also Figure S3.

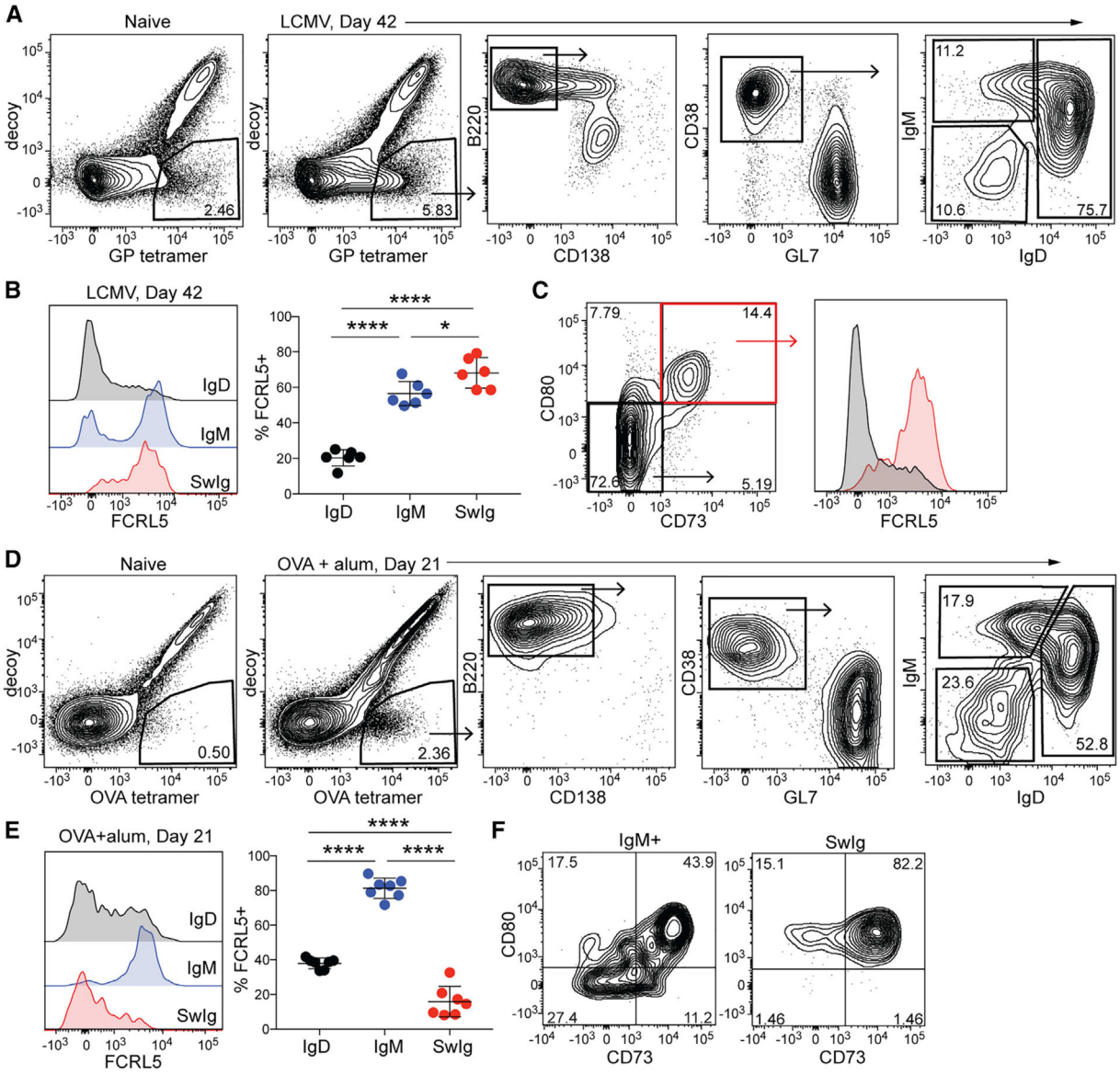

Figure 5. Acute Viral Infection and Protein Immunization Elicit FCRL5$^+$ MBCs

(A–C) Mice were infected for 6 weeks with LCMV Armstrong.

(A) Gating strategy to analyze MBCs specific for the LCMV glycoprotein (GP).

(B and C) FCRL5 expression was measured on GP-specific memory-naive cells (B220$^+$ CD38$^+$ CD138$^-$GL7$^-$) gated by (B) isotype or (C) expression of CD73 and CD80.

(D–F) Mice were immunized with OVA in alum, and splenocytes were analyzed 21 days later.

(D) Gating for OVA-specific MBCs.

(E and F) OVA-specific memory-naive cells were divided by isotype and analyzed for expression of FCRL5 (E) and CD80 and CD73 (F).

All graphs depict pooled results from two independent experiments, and each symbol represents an individual mouse. *p < 0.05; ***p < 0.001; ****p < 0.0001 by one-way ANOVA with Tukey's post-test.

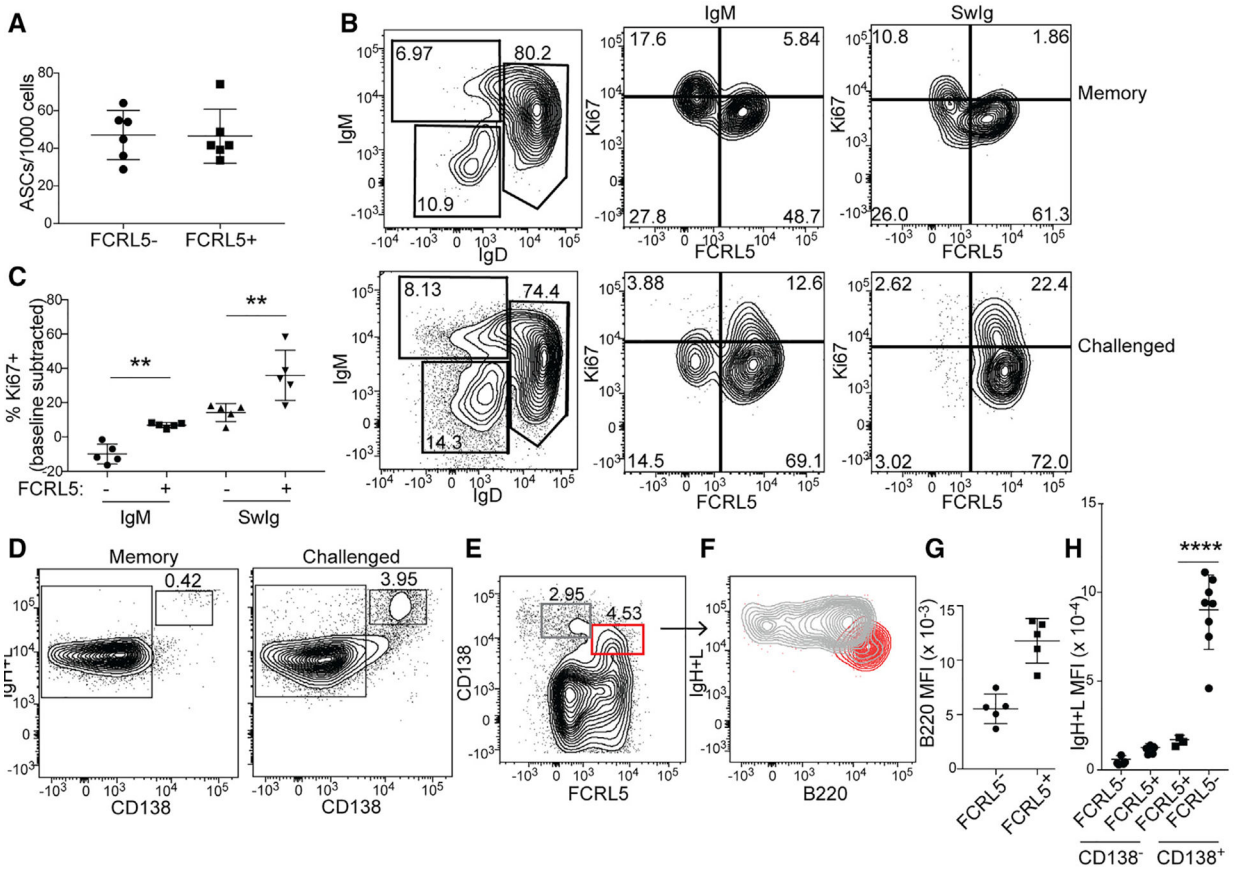

Figure 6. FCRL5^{+} MBCs Exhibit Robust Recall Responses

(A) FCRL5^{+} and FCRL5^{-}MSP1-specific MBCs (B220^{+} CD38^{+} CD138^{-}GL7^{-}IgD^{-}) were sorted from mouse spleens 3–4 months post-infection. Antibody- secreting cells (ASCs) were enumerated by EliSPOT after 3 days restimulation in interleukin-2 (IL-2) + R848.

(B–H) Four months after infection, mice were either challenged with 10^{7} *P. chabaudi* parasites or were not challenged (memory). MSP1-specific B cells were analyzed 5 days later.

(B) Representative flow plots of isotype distribution and Ki67 labeling in MSP1-specific MBCs (B220^{+} CD38^{+} CD138^{-}GL7^{-}) with or without challenge.

(C) Change in the percentage of IgM^{+} and SwIg MBCs expressing Ki67 after challenge, relative to % Ki67^{+} without challenge.

(D) Representative flow plots from memory and challenged mice showing the emergence of antibody-secreting cells (CD138^{+} IgH+L^{hi}) after challenge.

(E) FCRL5 expression on CD138^{int} and CD138^{hi} cells in challenged mice.

(F) Representative flow plot depicting expression of intracellular IgH+L and B220 on the populations defined in (E).

(G and H) Levels of B220 (G) and intracellular IgH+L (H) on the populations defined in (E). In (H), IgH+L expression in CD138^{-}B cells is shown for comparison. Two independent experiments were performed and pooled (A–H). Graphs depict mean ± SEM and symbols represent individual mice. **p < 0.01 by Mann-Whitney test (C). ****p < 0.0001 by one-way ANOVA with Tukey's post-test. See also Figure S4.

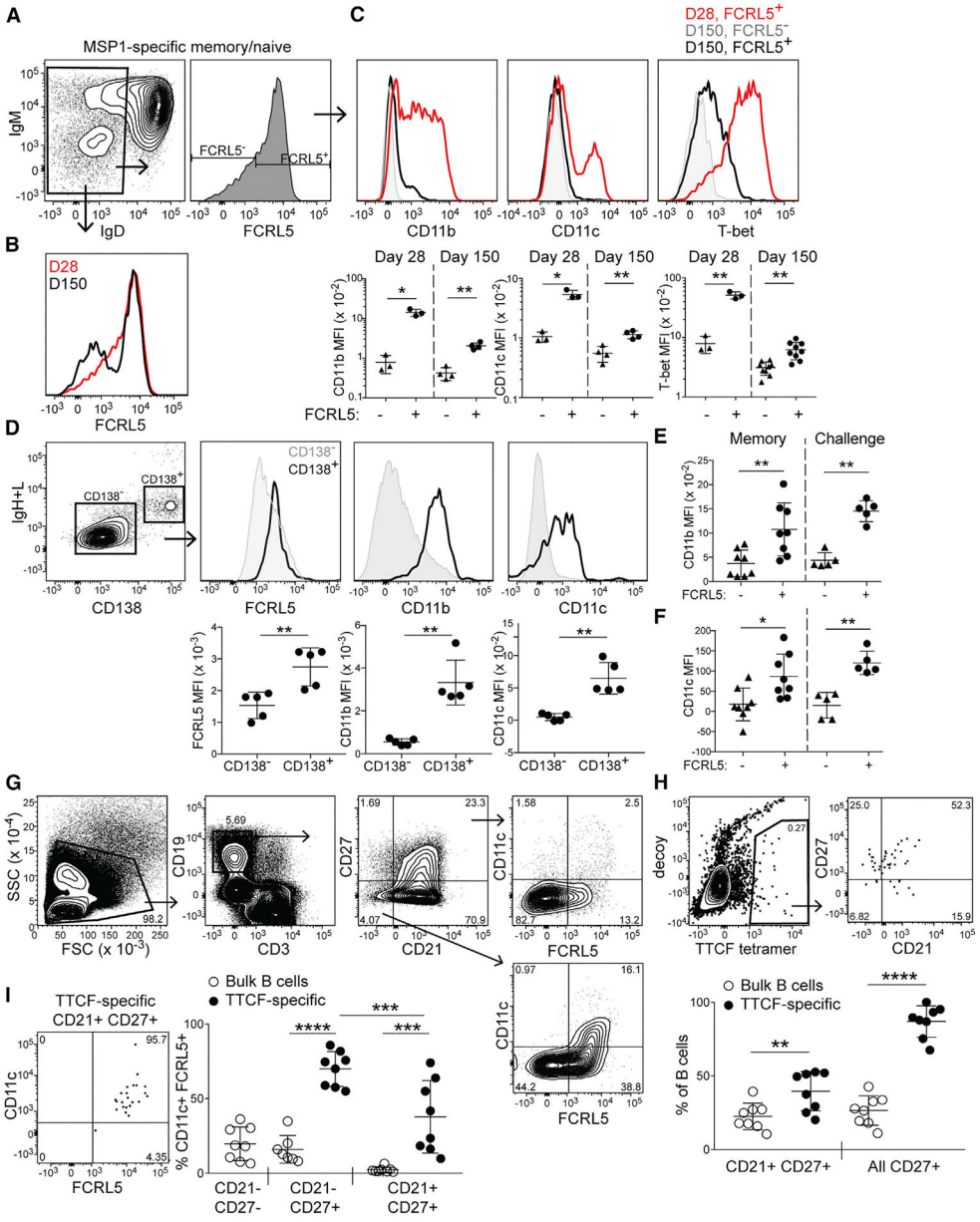

Figure 7. Long-Term Expression of Atypical Markers on MBCs in Mice and Humans

(A–F) Depict MSP1-specific B cells from mice infected with *P. chabaudi*.

(A) The memory-naive compartment ($B220^+$ $CD38^+$ $CD138^-GL7^-$) was further gated on IgD^-cells to enrich for MBCs and then divided into $FCRL5^+$ and $FCRL5^-$populations. Graphs show a representative sample from 28 d.p.i.

(B) Representative FCRL5 expression on IgD^-cells assessed 28 or 150 days post-infection.

(C) Histograms and quantification of CD11b, CD11c, and T-bet expression on the $FCRL5^+$ and $FCRL5^-$subsets defined in (A), from mice infected for 28 days (red) or 150 days (gray and black).

(D–F) Mice were infected for 150 days and then challenged with 10^7 parasites (challenge) or left unchallenged (memory). Splenocytes were harvested 3 days later.

(D) Expression of FCRL5, CD11b, and CD11c was assessed on MSP1-specific B cells from challenged mice. Antibody-secreting cells ($CD138^+$ intracellular $IgH+L^{hi}$) were compared to $CD138^-$cells.

(E and F) CD11b (E) and CD11c (F) were examined on MBCs ($B220^+$ $CD38^+$ $CD138^-GL7^-$ IgD^-) from both memory and challenged mice after gating into $FCRL5^+$ and $FCRL5^-$populations. Each symbol represents one mouse and all graphs depict pooled results from at least two independent experiments, except that day 28 data in (B) are from one representative experiment (of 3) that was performed side-by-side with a day 150 time point to show the direct comparison.

(G) Gating strategy for assessing atypical markers on bulk memory B cells from human peripheral blood. The stacked panels at right show expression of CD11c and FCRL5 on classical MBCs ($CD21^+$ $CD27^+$; top) and atMBCs ($CD21^-CD27^-$; bottom).

(H) Flow plots depict gating of CD21 and CD27 on tetanus toxoid-specific (TTCF) B cells. Graph shows the percentage of either total B cells (open circles) or TTCF-specific B cells (closed circles) that co-express CD27 and CD21, as well as the total frequency of $CD27^+$ cells irrespective of CD21 expression.

(I) Flow plot shows representative expression of FCRL5 and CD11c on TTCF-specific $CD21^+$ $CD27^+$ cells. Graph depicts the percentage of each indicated compartment that co-expresses FCRL5 and CD11c.

Data are pooled from 8 individual blood donors analyzed in 3 separate experiments; each symbol represents 1 donor. *$p < 0.05$; **$p < 0.01$; ***$p < 0.001$; ****$p < 0.0001$ by Mann-Whitney test (D–F) or one-way ANOVA with Tukey's post-test (H–I). See also Figures S5 and S6.

KEY RESOURCES TABLE

REAGENT or RESOURCE	SOURCE	IDENTIFIER
Antibodies (all anti-mouse unless specified)		
Anti-B220 (RA36-B2	BD	Cat# 563892; RRID:AB_2738470
Anti-CD138 (281-2)	Biolegend	Cat# 142516; RRID:AB_2562337
Anti-CD38 (90)	Biolegend	Cat# 102717; RRID:AB_2072892
Anti-GL7 (GL-7)	eBioscience	Cat# 485902-80; RRID:AB_10854881
Anti-IgM (RMM-1)	Biolegend	Cat# 406512; RRID:AB_2075943
Anti-lgD (1126c.2a)	Biolegend	Cat# 405731; RRID:AB_2563342
Anti-CD73 (eBioTY/11.8)	eBioscience	Cat# 250731-82; RRID:AB_10853348
Anti-CD80 (1610A1)	BD	Cat# 553769; RRID:AB_395039
Anti-FCRL5 (sheep polyclonal)	R&D	Cat# FAB6757G
Isotype Control (sheep polyclonal)	R&D	Cat# IC016G
Anti-CD4 (GK1.5)	eBioscience	Cat# 190041-82; RRID:AB_469533
Anti-CD8 (536.7)	BD	Cat# 553034; RRID:AB_394572
Anti-CD5 (537.3)	eBioscience	Cat# A15842; RRID:AB_2534612
Anti-CD1d (1B1)	eBioscience	Cat# 160011-81; RRID:AB_468837
Anti-CD11b (M1/70)	eBioscience	Cat# 140112-81; RRID:AB_467107
Anti-CD72a, b, d (K10.6)	BD	Cat# 740541; RRID:AB_2740247
Anti-CD86 (GL-1)	Biolegend	Cat# 105013; RRID:AB_439782
Anti-T-bet (eBio4B10)	eBioscience	Cat# 125825-80; RRID:AB_925762
Anti-Ki67 (SolA15)	eBioscience	Cat# 615698-80; RRID:AB_2574619
Anti-CD21 (4E3)	eBioscience	Cat# 570212-82; RRID:AB_657704
Anti-CD45.1 (A20)	BD	Cat# 560578; RRID:AB_1727488
Anti-CD45.2(104)	BD	Cat# 560696; RRID:AB_1727494
Anti-CD40 (FGK4.5)	UCSF Monoclonal Antibody Core	MyCores Item No. AM013
Anti-lgH+L (A11045)	Molecular Probes	Cat# A-11045; RRID:AB_142754
Anti-CD23 (B3B4)	eBioscience	Cat# 120232-82; RRID:AB_465593
Anti-CD11c (HL3)	BD	Cat# 553802; RRID:AB_395061
Anti-CD16/CD32 (2.4G2)	UCSF Monoclonal Antibody Core	MyCores Item No. AM004
Anti-human CD19 (HIB19)	BD	Cat# 555412; RRID:AB_395812
Anti-human IgD (IA62)	BD	Cat# 555776; RRID:AB_396111
Anti-human IgM (MHM-88)	Biolegend	Cat# 314521; RRID:AB_2561513
Anti-human CD21 (B-ly4)	BD	Cat# 555421; RRID:AB_395815
Anti-human CD27 (M-T271)	Biolegend	Cat# 356413; RRID:AB_2562504
Anti-human CD38 (HIT2)	BD	Cat# 560676; RRID:AB_1727472
Anti-human FCRL5 (509F6)	eBioscience	Cat# 503078-41; RRID:AB_2574198
Anti-human CD11 c (3.9)	Biolegend	Cat# 301641; RRID:AB_2564082
Anti-human CD20 (2H7)	BD	Cat# 560736; RRID:AB_1727451
Anti-human CD3 (UCHT1)	BD	Cat# 550368; RRID:AB_393639
Bacterial and Virus Strains		
LCMV Armstrong	M. Bevan (UW)	N/A
Biological Samples		
Healthy adult PBMCs-frozen	Bloodworks Northwest	Cat# 4580-03
Healthy adult PBMCs from apheresis-mobilized	D. Rawlings (SCRI)	N/A

REAGENT or RESOURCE	SOURCE	IDENTIFIER
TRIMA LRS Chambers	Bloodworks Northwest	Cat# 2490-08
Chemicals, Peptides, and Recombinant Proteins		
Ovalbumin	Sigma	Cat# A5503
Imject Alum	ThermoFisher	Cat# 77161
Streptavidin-APC or Streptavidin-PE	Prozyme	Cat# PJRS25 or PJ25S
Anti-APC or anti-PE magnetic beads	Miltenyi	130048-801 or 130090-855
MSP119	Krishnamurty et al., 2016	N/A
Tetanus Toxoid C Fragment	Expressed in-house	N/A
LCMV Glycoprotein	J. Teijaro	N/A
Critical Commercial Assays		
Transcription Factor Staining Buffer Set	eBioscience	005523-00
RNAqueous Micro Kit	Invitrogen	AM1931
Deposited Data		
RNA-Seq dataset	This paper	GEO: GSE85205
Experimental Models: Organisms/Strains		
Plasmodium chabaudi AS	MR4	#MRA-743
Plasmodium yoelii (17X NL)	MR4	#MRA-593
C57/BL6J mice	Jackson Labs	Stock #000664; RRID:IMSR_JAX:000664
CD45.1+ mice	Jackson Labs	Stock #002014; RRID:IMSR_JAX:002014
Ifngr1$^{-/-}$ mice	Jackson Labs	Stock #003288; RRID:IMSR_JAX:003288
Tbx21 fl/fl mice	Jackson Labs	Stock #022741; RRID:IMSR_JAX:022741
Mb1-Cre mice	M. Reth, Max Planck Institute	Jackson Stock #020505; RRID:IMSR_JAX:020505
Software and Algorithms		
RSEM 1.2.22	Li and Dewey, 2011	http://www.mybiosoftware.com/rsem-1-1-13-rna-seq-expression-estimation-expectation-maximization.html; RRID:SCR_013027
STAR 2.4.2a	Dobin et al., 2013	https://github.com/alexdobin/STAR/releases
DeSeq2	Love et al., 2014	DAhttps://bioconductor.org/packages/release/bioc/html/DESeq2.html; RRID:SCR_015687
DAVID	Dennis et al., 2003	https://david.ncifcrf.gov/; RRID:SCR_001881
Mouse Genome Informatics	Jackson Labs	http://www.informatics.jax.org/
Keisan Hypergeometric Probability Calculator	Casio Computer Co.	https://keisan.casio.com/exec/system/1180573201
Rothstein Lab Hypergeometric Probability Calculator	Rothstein lab	www.rothsteinlab.com/
I mage J	NIH	https://imagej.nih.gov/ij/; RRID:SCR_003070
Prism 7	GraphPad	https://www.graphpad.com/; RRID:SCR_002798
FlowJo 10	TreeStar	RRID:SCR_008520